Effect of ZrO_2 Nanoparticles on Thermophysical and Rheological Properties of Three Synthetic Oils

María J.G. Guimarey[a], Miguel R. Salgado[a], María J.P. Comuñas[a]*, Enriqueta R. López[a], Alfredo Amigo[b], David Cabaleiro[c,d], Luis Lugo[d], Josefa Fernández[a]

[a] *Laboratorio de Propiedades Termofísicas, Grupo NaFoMat, Departamento de Física Aplicada, Universidade de Santiago de Compostela, 15782 Santiago de Compostela, Spain*

[b] *Laboratorio de Propiedades Termofísicas y Superficiales de Líquidos, Departamento de Física Aplicada, Universidade de Santiago de Compostela, 15782 Santiago de Compostela, Spain*

[c] *Institute of Construction Technologies, National Research Council, 35127 Padova, Italy;*

[d] *Departamento de Física Aplicada, Facultade de Ciencias, Universidade de Vigo, 36310 Vigo; Spain*

[*] Corresponding author: M. J.P. Comuñas

E-mail address: mariajp.comunas@usc.es

ABSTRACT

This article presents an experimental study on some thermophysical properties (density, viscosity and adiabatic bulk modulus) of six synthetic oils-based ZrO_2 nanolubricants. Two-step method with ultrasonic disruptor was used to prepare the nanodispersions. The morphology, crystalline degree and elemental composition of nanoparticles were analyzed by electron microscopy. Visual observation, temporal variation of refractive index and dynamic light scattering were used to analyze the stability of the nanolubricants and the average size of the aggregates. The presence of new interactions between nanoparticles and base oils was studied through Fourier transform infrared spectrometer. Vibrating tube densimeters, rotational viscometer and rheometer equipped with cone-plate geometry were used within the temperature range from 278.15 to 373.15 K. The ability of some theoretical simple models to predict densities and viscosities of these nanolubricants as a function of temperature and nanoparticle concentration was also checked.

Keywords: synthetic oils; ZrO_2 nanoparticles; nanolubricants; adiabatic bulk modulus; density; rheology

1. **INTRODUCTION**

Lubrication is of great importance for the efficient use of machinery. The main purpose of lubrication is to reduce friction and wear in bearings or sliding components to prevent premature failure [1,2]. Frictional losses are the main source of energy loss in mechanical systems. It is crucial to investigate in the improvement of the thermophysical and tribological properties of lubricants which would lead to greater economic, social and environmental effectiveness. The variety of lubricating fluids has grown to satisfy the demands of new machines having more stringent requirements due to their operation under more severe conditions or in harsh environments [3]. Generally, the lubricants are formulated from synthetic, mineral or vegetable type base oils. Although mineral oils represent the majority of the market demand, many technological advances in equipment and machinery would not be possible without the benefits offered by synthetic oils [3]. To the base oils, additives are added (dissolved or suspended) to achieve the desirable characteristics of the final lubricant. Recently, Spikes published a review [4] to provide the state of art of friction modifier additives. Additives are organic or inorganic compounds that are used to improve properties (friction, viscosity grade and viscosity index, among others), to prevent wear and corrosion, or to reduce undesirable changes that appear during the service life of the lubricant (thermal degradation, for example). Hence, additives are used to improve the tribological performance of lubricants.

In recent years, numerous articles investigated the use of nanoparticles as oil additives [5,6]. Shahnazar et al. [7] have published a review that compiles the results of other researchers showing that lubricants containing nanoadditives may have better tribological properties than those including traditional additives. Xiao and Liu [8] have published a review remarking the recent developments in using 2D nanomaterials to improve the friction and the anti-wear properties of base lubricants [4,7,9-12]. Nanoadditive dispersions in base

oils are usually called nanolubricants [13]. A priori due to their thermal conductivity and high dynamic viscosity, nanolubricants will have good ability to tolerate shear force and to heat transfer [14]. The published works report studies on metals and their oxides [14-24], molybdenum and tungsten disulfide [8,25,26], metal borates [27,28], fullerenes [29,30], graphitic nanoparticles [25,31,32] and nanodiamond particles [33] as nanoadditives.

Representative properties such as viscosity, density, friction and wear coefficients, flow curves and thermal stability, among others, should be taken into consideration when evaluating lubricant performance. Then, it is necessary to study the effects of the nanoadditives on these properties. Hence, in this work we focus our attention on the thermophysical (density, speed of sound and adiabatic bulk modulus) and rheological properties (viscosity and flow curves) of six ZrO_2 nanolubricants based on three synthetic base oils (a polyalkyleneglycol, PAG2, a biodegradable polymeric ester, BIOE, and isotridecyl trimellitate, TTM). Some authors have previously studied the ability of ZrO_2 nanoparticles as lubricant additives. Thus, Hernández Battez et al. [16] have analyzed the antiwear behavior of ZrO_2 nanoparticles dispersed at mass concentrations of 0.5%, 1.0% and 2.0% in PAO6. The effect of ZrO_2 functionalized nanoparticles as additive of multialkylated cyclopentanes on the friction and wear behavior was investigated by Ma and Bai [34]. Rani et al. [35] have studied the tribological properties of ZrO_2 nanoparticles dispersed in a vegetable oil.

2. MATERIALS AND METHODS

2.1. Materials: characterization

We have used a dimethoxy-end-capped poly(propylene glycol) named as PAG2 that has been kindly provided by Croda. By using MALDI-TOF [36] mass spectrometry we have obtained for this fluid an average molecular mass, M_w, of 1717 g/mol, and a polydispersity

index M_w/M_n=1.022 [37] that indicates that this polymer can be considered as monodisperse. Taking into account that the molecular structure of this type of PAG is CH_3-O-[CH_2-$CH(CH_3)$-O]$_n$-CH_3, it can be concluded that, n, the average number of monomers is =29. The synthetic esters (isotridecyl trimellitate, TTM, and the biodegradable polymeric ester, BIOE) were provided by Verkol Lubricantes. General chemical structures of the three base oils are shown in Figure 1.

Zirconium oxide nanoparticles stabilized with 3% HfO_2 (30-60 nm nominal diameter and 5.9 $g \cdot cm^{-3}$ bulk density) with a purity of 99.9% were supplied by Iolitec (lot. INO059008). The ZrO_2 nanopowder was characterized by X-ray diffraction (XRD) using a Philips type powder diffractometer. The instrument was equipped with a graphite diffracted beam monochromator and copper radiation source ($\lambda(K\alpha 1)$=1.5406Å), operating at 40 kV and 30 mA. It is well known that ZrO_2 has three polymorphs [38]: monoclinic, tetragonal and cubic phases/structures. The X-ray patterns of ZrO_2 nanopowder present sharp and well defined peaks, evidence of a high degree of crystallinity as shown in Figure 2, where intensive diffraction patterns are observed at 2θ = 24.5º, 28.2º, 31.5º and 34.3º which correspond to monoclinic ZrO_2 crystal phase [39]. Monoclinic ZrO_2, baddeleyite, has the space group symmetry P21/c. The unit-cell dimensions are a = 0.5145 nm; b = 0.5210 nm; c = 0.5312 nm, and with angles $\alpha=\gamma$=90º and β=99.226º (ICSD 98-008-2545). These values are very close to the those of the literature [40].

The morphology and size of ZrO_2 nanoparticles were obtained by scanning electron microscopy (SEM, Zeiss FESEM Ultra Plus). As it is shown in Figure 3 these nanoparticles are spherical. Besides, with the help of an additional detector for energy dispersive X-ray microanalysis (EDX), the spectrum of ZrO_2 nanoparticles was obtained. As expected, results indicate the predominant presence of zirconium and oxygen in the sample. The content of hafnium is due to the manufacturer uses HfO_2 to stabilize the ZrO_2 nanoparticles. The

aggregation state of ZrO_2 nanoparticles dispersed in butanol was evaluated through transmission electron microscopy (TEM, JEOL JEM-2010) by using an accelerating voltage of 200 kV. Figure 4 reveals that ZrO_2 nanoparticles appear as aggregates of individual particles.

2.2. Nanolubricant Preparation

Two-step method was used to prepare the nanolubricants. Firstly, we mixed the ZrO_2 nanoparticles, in form of dry powder, with the base oil (PAG2, TTM or BIOE). A high precision balance Sartorius MC 210P was used to determine the mass concentration of ZrO_2 nanoparticles (around 1 wt % or 2 wt %, which correspond to 0.17% and 0.34% in volume fraction, considering a density value of 5.9 $g \cdot cm^{-3}$ for the ZrO_2 nanopowder). The readability of the balance in the measured mass range is 0.00001 g. Secondly, we disperse the nanoparticles in the base oil by using an ultrasonic disruptor (HD 2200 Sonopuls). The sonicator probe conducts the acoustic energy from the transducer into the sample. The energy transferred to the nanodispersion depends on: the applied power, the total time that the dispersion is subjected to ultrasounds, the volume of the sample, the shape and diameter of the probe and its immersion depth. In this work we have used the same power (200 W), amplitude (302 μm), diameter and shape probe (MS73, 3 mm), sonication time (30 minutes) and prepared the same sample volume (20 ml) for all studied nanolubricants. To minimize overheating during sonication, the samples were immersed in an ice-water bath. Fourier transform infrared spectrometer (FTIR, VARIAN 670-IR) analyses were conducted to study the formation of chemical bonds between nanoparticles and the base oils. FT-IR spectra of PAG2, TTM and BIOE base oils and their corresponding nanodispersion at 2 wt % are shown in Figure 5. For pure PAG2 typical bands [41,42] are visible at wavenumbers of 2867 cm^{-1} (CH_2 stretching), 1373 cm^{-1} (CH_3 bending) and 1093 cm^{-1} (C-O-C asymmetrical stretching).

For TTM typical bands appears at 2956, 2925 and 2871 cm^{-1} (C-H stretching), 1725 cm^{-1} (C=O stretching), 1461 (aromatic C=C stretching), 1234, 1112 and 1068 cm^{-1} (C-O stretching) [43]. For BIOE typical bands [44] take place at 2921 cm^{-1} and 2852 cm^{-1} which conform to -CH_2 asymmetrical and symmetrical stretching respectively, 1743 cm^{-1} which confirms the formation of ester linkages in the methyl ester of the oil, and 1151 cm^{-1} which corresponds to a C-O link typical of esters. No new spectral peaks or shifts are found for the dispersions in comparison with the base oils, which indicates that no chemical bonds were formed.

Visual observation is the simplest method to initially evaluate stability of nanolubricants. In this work, the nanolubricants were placed at room temperature without any disturbance. Subsequently, the samples were observed every hour until detecting the nanoparticles sedimentation at the bottom of the container. Figure 6 shows photographs of the ZrO_2 nanoparticles dispersed in PAG2, TTM or BIOE as a function of the time for the dispersions prepared at the highest nanoparticle concentration. From the visual analysis it can be observed that dispersion based on BIOE base oil showed the fastest sedimentation. Separation layer of ZrO_2 and base lubricant (BIOE) can be clearly seen 144 hours after sonication. Partially sedimentation appears after 48 h for the other two nanolubricants based on visual tests but the separation layer is not clearly observed at 192 h. For all nanolubricants prepared in this work the time interval necessary to visually observe partial sedimentation is much higher than that necessary to perform the thermophysical experiments (3 hours). In order to use a less qualitative method to analyze the stability of the nanolubricants we have performed some tests with an UV-Vis spectrophotometer (Varian Cary 50 Bio UV-Visible) and a turbidimeter (Hanna Instruments HI 88713). UV-Vis spectrophotometry is one of the most common techniques employed to investigate the stability of colloidal suspensions. Nevertheless, at the concentrations of interest (1 wt % and 2 wt %) signals from both devices

show saturation (dispersions are usually too opaque so that the absorbance and the turbidity cannot be analyzed). Thus, it was necessary to dilute the dispersions up to a mass concentration around 10^{-3} wt %. In our opinion, it is not rigorous to extrapolate the results found for 10^{-3} wt % to 2 wt %, and therefore both techniques have been discarded.

We have also used dynamic light scattering (Zetasizer Nano ZS DLS) due to this technique offers the possibility of obtaining the average size of dispersed nanoparticles as well as valuable information of the stability of dispersions. For PAG2-based nanofluids we have obtained average diameters of 226 nm and 234 nm for 1 wt % and 2 wt % concentrations, respectively. For nanolubricants based on TTM, the mean diameters are 102 nm and 87 nm and for those based on BIOE 67 nm and 69 nm. As a result, DLS data reveal agglomeration of ZrO_2 nanoparticles in the suspensions, the lowest agglomeration corresponding to the dispersions containing BIOE whereas for PAG2-based nanofluids the average cluster size is around four times the diameter of the primary ZrO_2 nanoparticles. We observed that the highest average diameter was obtained for the base oil with the lowest viscosity grade (PAG2). This may be due to smaller probability of collision of nanoparticles in the more viscous fluids because a lower Brownian motion. Moreover, in the more viscous fluids can suspend particles easier because the higher hydrodynamic drag. Figure 7 represents the temporal evolution of the average diameter for the nanofluids at 2 wt %. The three nanolubricants present partial sedimentation at the initial stage (within 24 hours after sonication). This time interval is shorter that those estimated only from visual tests, but larger than those needed to measure the thermophysical properties.

Furthermore, we have checked the possibility to use a refractometer (Mettler Toledo RA-510M) to analyze the stability of the nanolubricants. Thus, the temporal evolution of the refractive index (n) at 298.15 K has been registered over 99 hours for ZrO_2/PAG2 and ZrO_2/TTM nanolubricants at 2 wt %. For BIOE based nanolubricants it was not possible to

make this study due to its refractive index is outside the instrument working range. The interest of this study is not the quantitative value of the refractive index but its time dependence. For each nanolubricant, we have performed three replicates of the temporal evolution of the refractive index. That is, we sonicate the samples at the conditions detailed above (power, amplitude and sonication time), after that we measure the refractive index as a function of time. Several days later, we sonicate again the sample (under the same conditions) and we measure again the temporal dependence of *n*. As Figure 8 shows, 20 hours after sonication the refractive index increases with time for both PAG2 and TTM-based nanolubricants, which could mean that nanoparticle sedimentation occurs. Another interesting fact we observe for nanolubricants containing PAG2 is that the $n(t)$ curve is practically the same for the three test performed, even if for one of them we have sonicated 120 minutes instead of 30 minutes as usual. This is not the case of TTM based nanolubricants, for which we observe different curves for each sonication process. This fact could mean that the agglomeration is more sensible to the sonication process for this last nanolubricant. Indirectly this fact could also be affected by the high viscosity of TTM base oil (1449 mPa·s at 293.15 K against 143 mPa·s for PAG2). The overall variation of the refractive index is smooth (≤ 0.003) during the 20 first hours after sonication for both PAG2 and TTM based nanolubricants. This result could confirm that these nanolubricants are relatively stable during this time interval.

2.3. Thermophysical characterization techniques

Density at atmospheric pressure of the nanolubricants was measured by using a vibrating densimeter Anton Paar SVM 3000 Stabinger. We have performed the measurements from 278.15 to 373.15 K. The temperature of the cell is controlled through an integrated thermostat with cascaded Peltier elements and measured with a Pt100

thermometer with an uncertainty of 0.02 K. The density measuring cell works on the proven principle of the oscillating tube. Density cell is a glass U-tube, which is excited to produce mechanical resonant vibrations according to DIN 51757 standard. The expanded (k=2) uncertainty of density measurements performed with SVM 3000 Stabinger is 0.0005 $g \cdot cm^{-3}$. Density values obtained directly from mechanical oscillator densimeters do not often include the effect that the sample viscosity has on the measurement. In such cases, it is necessary to apply a correction factor. Anton Paar SVM 3000 Stabinger reports directly the corrected density value. To check the consistency of the measurements, density of nanolubricants has also been measured with another vibrating tube densimeter (Anton Paar DSA 5000) that can work at 0.1 MPa from 283.15 to 338.15 K. The expanded uncertainty (k=2) of density measurements performed with DSA 5000 is 0.00001 $g \cdot cm^{-3}$. The speed of sound was also measured by using this device from 283.15 to 338.15 K, with an expanded uncertainty (k=2) of 1 $m \cdot s^{-1}$.

Viscosity at atmospheric pressure was measured also with the Anton Paar Stabinger SVM 3000 rotational viscometer. This apparatus allows measuring dynamic and kinematic viscosities from 278.15 to 373.15 K, in a viscosity range from 0.2 mPa·s to 20 Pa·s. The SVM 3000 Stabinger viscometer has a cylindrical geometry and it is based on a modified Couette principle with a rapidly rotating outer tube and an inner measuring bob that rotates more slowly. Experimental expanded uncertainty of 1% has been estimated for dynamic viscosity. The rheological behavior of the nanolubricants was studied by using a rotational rheometer (Physica MCR 101, Anton Paar), equipped with a cone-plate geometry with a cone diameter of 25 mm and a cone angle of 1°. The measurement procedure consists of imposing shear stress to the sample and recording the corresponding shear rate. Temperature is controlled with an uncertainty of 0.02 K with a Peltier P-PTD 200 system/device placed at the lower plate. We have performed the flow curves at 283.15, 303.15 and 323.15 K.

3. RESULTS AND DISCUSSION

Densities obtained for the base oils with SVM 3000 Stabinger and DSA 5000 densimeters are reported in Table 1. PAG2 has the highest density followed by TTM and finally by BIOE. Average absolute deviations (AAD%) between the values obtained with Stabinger densimeter and those of DSA 5000 are 0.05% for PAG2 and BIOE, and 0.04% for TTM. The values obtained with Stabinger densimeter for the three base oils have also been compared with those densities previously published by Otero et al. [45] and by Paredes [46]. Figure 9 shows AADs lower than 0.06% for PAG2 and 0.04% for both TTM and BIOE. These results confirm the good agreement between the density values obtained in this work for the three base oils and previous literature data. We have also compared the density data reported in Table 1 for PAG2 with those previously published by Fandiño et al. [37]. The average deviation is 0.02% for the data obtained from Stabinger densimeter and 0.05% for those determined by DSA 5000 apparatus. These deviations confirm the excellent agreement with Fandiño et al. [37] data.

Density values obtained with SVM 3000 Stabinger and DSA 5000 for all the nanolubricants are reported in Tables 2 and 3, respectively. Figure 10 confirms that density of all nanolubricants increases with the mass concentration of ZrO_2 nanoparticles. Data reveals that studied ZrO_2 nanofluids at 1 and 2 wt % produces an increase on the density of the three base oils around 0.7% and 1.8%, respectively. Density data determined with SVM 3000 Stabinger for nanodispersions are in agreement with those provided by Anton Paar DSA 5000. Thus, AADs of 0.04% and 0.03% were found for ZrO_2/PAG2 nanofluids at 1 wt % and 2 wt %, respectively. Similarly, AAD values are 0.07% and 0.04% for ZrO_2/TTM and 0.03% for ZrO_2/BIOE samples. We must point out that another difficulty that we have found in the experimental density determination is that the ZrO_2 nanoparticles adhered to the glass cell of the vibrating tube densimeters. Figure 11 shows a photograph of the glass cell

of the Stabinger densimeter before and after carrying out the measurements. This fact must be taken into account for future investigations with ZrO_2 nanoparticles and experimental devices based on glass cells.

The results obtained for the speed of sound of the neat base oils are reported in Table 4. PAG2 presents the lowest values (around 1382 $m \cdot s^{-1}$) followed by TTM (1508 $m \cdot s^{-1}$) and finally by BIOE (around 1523 $m \cdot s^{-1}$), in the three cases at the temperature of 283.15 K. The speed of sound values of pure TTM and BIOE at 313.15 K are close to those found by Mia and Ohno [47] for other ester oils. Table 5 gathers the measured speed of sounds for all ZrO_2 nanolubricants. For the three designed nanolubricant sets, temperature seems to exhibit a more significant influence on the speed of sound than the mass nanoparticle concentration. Thus, this property reduces around 2.5% with a 10 K temperature increase (13% in the entire temperature range), while only a reduction of 1% was found for the 2 wt % concentration of nanoparticles compared to the base lubricants. From the speed of sound and density data, the adiabatic bulk modulus (K_S) or adiabatic compressibility (κ_S) can be obtained from the relations:

$$K_S = \rho u^2 = 1/\kappa_S \quad (1)$$

Ohno et al. [48] remark that the bulk modulus of lubricating oils is a predominant factor affecting traction behavior in high-pressure elastohydrodynamic contacts. Thus, Mia [49] investigated the use of the adiabatic bulk modulus as predictive parameter for pressure-viscosity coefficient of oils. This coefficient is essential to evaluate the performance of lubricating oils under elastohydrodynamic lubrication regime. Mia and Ohno [47] also observed that lubricating oils with low values of adiabatic bulk modulus present good low temperature fluidity. In this work, we have determined the adiabatic bulk modulus for the three base oils as well as for the ZrO_2 nanolubricants. The lowest values of the adiabatic bulk

modulus are found for PAG2 and then, as expected, for ZrO_2/PAG2 nanolubricants. Synthetic esters and their nanolubricants present higher adiabatic bulk modulus. In Figure 12 it can be observed that the adiabatic bulk modulus has a smoothly variation with the addition of ZrO_2 nanoparticles. Thus, variations around 0.5% were found for all the nanolubricants over all the entire temperature range. From these results and the previous remarks of Mia and Ohno [47] we can conclude that the nanolubricants with the better low temperature fluidity will be those based on PAG2.

Flow curves for base oils and the nanolubricants were analyzed by using a rotational rheometer (Physica MCR 101, Anton Paar). Figure 13a shows the shear stress-shear rate dependence for the pure base oils at 283.15 and 303.15 K. The shear stress is linear with the shear strain rate for the three synthetic oils up to 10000 s^{-1} entailing Newtonian behavior at these conditions. The significant decrease in shear stress with the temperature due to the weakening of the intermolecular attraction with the rise of temperature is also observed. The linear relationship found in the flow curves for the base oils remains present when ZrO_2 nanoparticles are dispersed at 1 wt % and 2 wt % concentration up to 1000 s^{-1} (Figure 13b). However, in tribological applications such as bearings and gears, lubricants are subject to very high strain rates on the order of 10^7 s^{-1} and under these conditions, even relatively low-molecular-weight fluids exhibit shear thinning behavior [50]. This kind of experimental rheological measurement requires ultra-shear viscometers, as those performed by Hernández Battez et al. [50]. Thus these authors observed for PAO6 and nanofluids based on PAO6, a non-Newtonian shear thinning behaviour with varying trends at higher shear rates (10^6-10^7 s^{-1}). Recently Meyer et al. [51] have reviewer the non-Newtonian behaviour of nanofluids. Therefore, we can assert that all the samples analyzed here behave like Newtonian fluids over the studied conditions. The dynamic viscosities of the pure base oils are reported in Table 6. The synthetic esters (BIOE and TTM) are significantly more viscous than PAG2,

especially at low temperatures, being this fact in agreement with the cited above conclusions derived from bulk modulus trend. The viscosities obtained with the Stabinger rotational viscometer for the three base oils have also been compared with those values previously published by Otero et al. [45] for TTM and BIOE and by Paredes et al. [52] for PAG2. The obtained AADs, showing good agreements, are 0.1% for PAG2, 0.7% for TTM and 1.7% for BIOE. Figure 14 shows the temperature dependence of the viscosity for the three base oils. A diminution around 330 mPa·s is found for PAG 2 over the entire temperature range, being this value around 6500 and 5500 mPa·s for TTM and BIOE, respectively. As can be observed in Table 7, dynamic viscosities increase with nanoparticle concentration, being ZrO_2 /TTM at concentration of 2 wt % the most viscous of the studied samples.

For the regression of the experimental viscosity data we have used the following expression:

$$\eta(T) = A\exp\left(\frac{B}{T-C}\right) \tag{2}$$

The parameter values (A, B and C) are reported in Table 8. This equation reproduces the experimental values with AAD% lower or equal than 0.2%, 1% and 3.7% for PAG2, BIOE and TTM based nanolubricants, respectively. Figure 15 shows the variation of viscosity with the concentration of nanoparticles at 278.15 K, 323.15 K and 373.15 K. For PAG2 based nanolubricants the increase in viscosity due to nanoparticle addition is around (4 – 5) % over the whole temperature interval, being these values (6 – 8) % and (3 – 4) % for TTM and BIOE nanolubricants, respectively. These results can be compared with those found in the literature for other nanolubricants. Thus, a three times increase in viscosity was observed by Kole and Dey [53] with the addition of 2.5% volume fraction of CuO nanoparticles in a gear oil. Kotia and Gosh [19] observed an increment of 10.5% with 0.5% Al_2O_3 particle volume fraction in other gear oil.

We have also analyzed the ability of some simple equations to model densities and viscosities of the nanolubricants studied in this work. Thus, for density, ρ, we have used the following expressions due to Pak and Cho [54] and Wasp et al. [55], respectively:

$$\rho_{nf} = (1-\phi)\,\rho_{bf} + \phi\rho_{np} \tag{3}$$

$$\frac{1}{\rho_{nf}} = \frac{1-\varphi}{\rho_{bf}} + \frac{\varphi}{\rho_{np}} \tag{4}$$

where subscripts nf, bf and np stand for nanofluid, base oil and bulk ZrO_2, respectively, and ϕ and φ are the volume and mass fractions of the nanoadditive, respectively. Both equations are widely used [56,57] to estimate density of nanofluids. As Figure 16a shows, densities predicted with both equations agree well with experimental values, thus AADs lower than 0.08% with the Pak and Cho [54] model and lower than 0.12% with the Wasp et al. [55] equation were found for all nanolubricants.

Mishra et al. [58] have published a summary of the viscosity models that can be applied for nanofluids. Recently, Barati-Harooni et al. [59] remark that the development of accurate models for the prediction of the viscosity of nanofluids is of great importance. These authors [59] analyze the use of several empirical equations [60-64] to describe the viscosity of nanofluids (mainly developed for thermal applications) containing water, ethylene glycol or propylene glycol as base fluids, and metallic oxide nanoparticles, carbon nanotubes and graphene as additives. In the present work we have evaluated the goodness of some of these equations to model the viscosity of the studied ZrO_2 nanolubricants. Thus, the following expression suggested by Einstein [62] was used:

$$\eta_{nf} = (1+2.5\phi)\,\eta_{bf} \tag{5}$$

where η_{nf} is the nanofluid viscosity, η_{bf} is the base oil viscosity and ϕ is the volume fraction of the nanoadditive. The AADs between experimental viscosities from Table 7 and those predicted by using equation (5) are 2-3% for the nanolubricants based on PAG2 and BIOE,

being 4-6% these values for ZrO_2/TTM samples. We have observed that this equation underpredicts the viscosity of the nanolubricants. It is necessary to highlight that Einstein equation is valid for dilute non-interacting suspensions of spherical particles. We have also tried to use the following empirical equations due respectively to Saito (equation 6), Brinkman (equation 7), Batchelor (equation 8), Wang et al. (equation 9) and Chen et al. [60,61,64-66]:

$$\eta_{nf} = (1 + \frac{2.5\phi}{1 - \phi})\ \eta_{bf} \tag{6}$$

$$\eta_{nf} = \frac{1}{(1-\phi)^{2.5}}\ \eta_{bf} \tag{7}$$

$$\eta_{nf} = \left(1 + 2.5\phi + 6.2\phi^2\right) \eta_{bf} \tag{8}$$

$$\eta_{nf} = \left(1 + 7.3\phi + 123\phi^2\right) \eta_{bf} \tag{9}$$

$$\eta_{nf} = \left(1 + 10.6\phi + (10.6\phi)^2\right) \eta_{bf} \tag{10}$$

These equations (5 to 10) are the most frequently applied in theoretical or empirical models for viscosity estimation of nanofluids. As it can be seen in Figure 16b the highest AADs were found for nanolubricants based on TTM oil. The results obtained with Saito [65], Brinkman [61] and Batchelor [60] equations are quite similar to those obtained with Einstein equation. For PAG and TTM based nanolubricants we observe that the deviations between the predicted and the experimental viscosity values increase with the concentration of nanoparticles for all the empirical equations used. For BIOE based nanolubricants the deviations remain almost constant (around 3%) with nanoparticles concentration for equations 5 to 8. However, with equations 9 and 10 the deviations decrease with concentration. The best results were obtained with the Chen et al. model [64] (equation 10),

for which AADs ranges from (0.29 to 0.33%) for PAG2 based nanolubricants, from (2.27 to 3.52%) for TTM nanolubricants and (0.50 to 1.54%) for BIOE based nanolubricants.

4. CONCLUSIONS AND FUTURE WORK

Experimental studies of different additives and base oils combinations are needed to analyze the influence that nanoadditives have on the thermophysical properties, and subsequently to elucidate lubricating mechanism with nanoadditives. In this work we have observed that the nanolubricant dispersion stability was low and the ZrO_2 nanoparticles started to suspend so early after sonication. Results show that density increases (around 2%) with the increase of the mass concentration of ZrO_2 nanoparticles. The same occurs with viscosity for which increments up to 8% are observed for isotridecyl trimellitate ester based nanolubricants. Adiabatic bulk modulus has a smoothly variation with the addition of zirconium oxide nanoparticles. The best low temperature fluidity was observed for nanolubricants containing poly(propylene glycol). Linearity found in the flow curves of the three base oils is also present when nanoparticles are added; this fact confirms the Newtonian behavior of all the nanolubricants studied in this work at shear strain rates up to 1000 s^{-1}. The predicted densities agree with the experimental data being the average absolute deviations lower or equal than 0.12%. For viscosities the Chen et al. predictive model showed reasonably agreement (absolute relative deviations lower than 4%) with the experimental viscosity data. In a future it will be interesting to analyze if the usage of dispersants or nanoparticle functionalization could improve the stability of these nanolubricants. Finally, we must point out that more efficient techniques for dispersing nanoadditives in base oils and for controlling the stability of the nanodispersions are still necessary.

NOMENCLATURE

M_w	Molecular mass ($g \cdot mol^{-1}$)
n	Refractive index
T	Temperature (K)
p	Pressure (Pa)
ρ	Density ($g \cdot cm^{-3}$)
ρ_{np}	Density of nanoparticle ($g \cdot cm^{-3}$)
ρ_{bf}	Density of the base oil ($g \cdot cm^{-3}$)
ρ_{nf}	Density of nanofluid ($g \cdot cm^{-3}$)
u	Speed of sound ($m \cdot s^{-1}$)
K_s	Adiabatic bulk modulus (GPa)
κ_s	Adiabatic compressibility (GPa^{-1})
α	Pressure-viscosity coefficient
$\dot{\gamma}$	Shear rate (s^{-1})
τ	Shear stress (Pa)
η	Viscosity (Pa·s)
η_{bf}	Viscosity of the base oil (Pa·s)
η_{nf}	Viscosity of nanofluid (Pa·s)
τ	Shear stress (Pa)
ϕ	Particle volume fraction
φ	Particle mass fraction
AAD	Average absolute deviations

SUBSCRIPTS

np	Nanoparticle

bf Base fluid

nf Nanofluid

ACKNOWLEDGMENTS

Authors acknowledge Croda and Verkol Lubricantes for the lubricants provided. This work was supported by Spanish Ministry of Economy and Competitiveness and the UE FEDER programme through ENE2014-55489-C2-1-R, ENE2014-55489-C2-2-R, ENE2017-86425-C2-1-R and ENE2017-86425-C2-2-R projects. Moreover, this work was funded by the Xunta de Galicia (AGRUP2015/11 and GRC ED431C 2016/001). D.C. was recipient of a postdoctoral fellowship from Xunta de Galicia (Spain).

REFERENCES

[1] N.S. Ahmed, A.M. Nassar, Lubrication and Lubricants, Tribology-Fundamentals and Advancements, InTech, 2013.

[2] Y. Zhang, Boundary lubrication—An important lubrication in the following time, J. Mol. Liquids 128 (2006) 56-59.

[3] L.R. Rudnick, Synthetic, Mineral Oils and Bio-based Lubricants (2013).

[4] H. Spikes, Friction Modifier Additives, Tribol. Lett. 60 (2015) 1-26.

[5] M. Ivanov, O. Shenderova, Nanodiamond-based nanolubricants for motor oils, Curr. Opin. Solid St. M. 21 (2017) 17-24.

[6] L. Kong, J. Sun, Y. Bao, Preparation, characterization and tribological mechanism of nanofluids, RSC Advances 7 (2017) 12599-12609.

[7] S.Shahnazar, S.B.A. Bagheri, Enhancing lubricant properties by nanoparticle additives, Int. J. Hyd. Energy 41 (2016) 3153-3174.

[8] H. Xiao, S. Liu, 2D nanomaterials as lubricant additive: A review, Materials & Design 135 (2017) 319-332.

[9] V.N. Bakunin, A.Y. Suslov, G.N. Kuzmina, O.P. Parenago, Recent Achievements in the synthesis and application of the inorganic nanoparticles as lubricant components- a Review, Lubr. Sci. 17 (2005) 127-145.

[10] B. Gupta, N. Kumar, K. Panda, S. Dash, A.K. Tyagi, Energy efficient reduced graphene oxide additives: Mechanism of effective lubrication and antiwear properties, Sci. Rep. 6 (2016) 18372.

[11] G. Zhao, Q. Zhao, W. Li, X. Wang, W. Liu, Tribological properties of nano-calcium borate as lithium grease additive, Lubr. Sci. 26 (2014) 43-53.

[12] J.M. Martin, N. Ohmae, Nanolubricants vol. 13, Wiley, New York (2008).

[13] L. Joly-Pottuz, Nanolubricants. in: Q.J. Wang, Y.-W. Chung, (Eds.), Encyclopedia of Tribology, Springer US, Boston, MA, 2013, pp. 2364-2369.

[14] M. Hemmat Esfe, M.R. Sarlak, Experimental investigation of switchable behavior of CuO-MWCNT (85%–15%)/10W-40 hybrid nano-lubricants for applications in internal combustion engines, J. Mol. Liquids 242 (2017) 326-335.

[15] R. Chou, A.H. Battez, J.J. Cabello, J.L. Viesca, A. Osorio, A. Sagastume, Tribological behavior of polyalphaolefin with the addition of nickel nanoparticles, Tribol. Int. 43 (2010) 2327-2332.

[16] A. Hernández-Battez, R. González, J.L. Viesca, J.E. Fernández, J.M.D. Fernández, A. Machado, R. Chour, J. Riba, CuO, ZrO_2 and ZnO nanoparticles as antiwear additive in oil lubricants, Wear 265 (2008) 422-428.

[17] A. Hernández-Battez, R. Gonzalez, D. Felgueroso, J.E. Fernandez, M.R. Fernández, M.A. García, I. Penuelas, Wear prevention behaviour of nanoparticles suspension under extreme pressure conditions, Wear 263 (2007) 1568-1574.

[18] A. Hernández-Battez, J.E.F. Rico, A. Navas, J.L. Viesca, R. Chou, J.M. Diaz, The tribological behaviour of ZnO nanoparticles as an additive to PAO6, Wear 261 (2006) 256-263.

[19] A. Kotia, S.K. Ghosh, Experimental analysis for rheological properties of aluminium oxide (Al_2O_3)/gear oil (SAE EP-90) nanolubricant used in HEMM, Ind. Lub. Tribol. 67 (2015) 600-605.

[20] Q. Xue, W. Liu, Z. Wang, Friction and wear properties of a surface-modified TiO_2 nanoparticle as an additive in liquid paraffin, Wear 213 (1997) 29-32.

[21] Z.S. Hu, J.X. Dong, G.X. Chen, Study of antiwear and reducing friction additive of nanometer ferric oxide, Tribol. Int. 31 (1998) 355-360.

[22] K. Sepyani, M. Afrand, M. Hemmat Esfe, An experimental evaluation of the effect of ZnO nanoparticles on the rheological behavior of engine oil, J. Mol. Liquids 236 (2017) 198-204.

[23] S. Kannaiyan, C. Boobalan, A. Umasankaran, A. Ravirajan, S. Sathyan, T. Thomas, Comparison of experimental and calculated thermophysical properties of alumina/cupric oxide hybrid nanofluids, J. Mol. Liquids 244 (2017) 469-477.

[24] M. Karimi-Nazarabad, E.K. Goharshadi, A. Youssefi, Particle shape effects on some of the transport properties of tungsten oxide nanofluids, J. Mol. Liquids 223 (2016) 828-835.

[25] M. Farsadi, S. Bagheri, N.A. Ismail, Nanocomposite of functionalized graphene and molybdenum disulfide as friction modifier additive for lubricant, J. Mol. Liquids 244 (2017) 304-308.

[26] L. Joly-Pottuz, F. Dassenoy, Nanoparticles Made of Metal Dichalcogenides, Nanolubricants, John Wiley & Sons, Ltd, 2008, pp. 15-92.

[27] C. Boshui, G. Kecheng, F. Jianhua, W. Jiang, W. Jiu, Z. Nan, Tribological characteristics of monodispersed cerium borate nanospheres in biodegradable rapeseed oil lubricant, Appl. Surf. Sci. 353 (2015) 326-332.

[28] Z.S. Hu, R. Lai, F. Lou, L.G. Wang, Z.L. Chen, G.X. Chen, J.X. Dong, Preparation and tribological properties of nanometer magnesium borate as lubricating oil additive, Wear 252 (2002) 370-374.

[29] T. Jafari Behbahani, A.A.M. Beigi, Z. Taheri, B. Ghanbari, The effect of amino [60] fullerene derivatives on pour point and rheological properties of waxy crude oil, J. Mol. Liquids 211 (2015) 308-314.

[30] J. Lee, S. Cho, Y. Hwang, H.-J. Cho, C. Lee, Y. Choi, B.-C. Ku, H. Lee, B. Lee, D. Kim, S.H. Kim, Application of fullerene-added nano-oil for lubrication enhancement in friction surfaces, Tribol. Int. 42 (2009) 440-447.

[31] E.K. Goharshadi, Z. Niyazi, M. Shafaee, M.B. Moghaddam, R. Ludwig, M. Namayandeh-Jorabchi, Transport properties of graphene quantum dots in glycerol and distilled water, J. Mol. Liquids 241 (2017) 831-838.

[32] A.K. Rasheed, M. Khalid, W. Rashmi, T.C.S.M. Gupta, A. Chan, Graphene based nanofluids and nanolubricants – Review of recent developments, Renew. Sustain. Energy Rev. 63 (2016) 346-362.

[33] M.G. Ivanov, D.M. Ivanov, Nanodiamond Nanoparticles as Additives to Lubricants, Ultananocrystalline Diamond Second Edition (2012).

[34] J. Ma, M. Bai, Effect of ZrO_2 Nanoparticles Additive on the Tribological Behavior of Multialkylated Cyclopentanes, Tribol. Lett. 36 (2009) 191-198.

[35] S. Rani, The tribological behavior of TiO_2, CeO_2 and ZrO_2 nano particles as a lubricant additive in rice bran oil, Int. J. Sci. Eng. Res. 7 (2016) 708-712.

[36] H.J. Räder, W. Schrepp, MALDI-TOF mass spectrometry in the analysis of synthetic polymers, Acta Polymer. 49 (1998) 272-293.

[37] O. Fandiño, L. Lugo, M.J.P. Comuñas, E.R. López, J. Fernández, Temperature and pressure dependences of volumetric properties of two poly(propylene glycol) dimethyl ether lubricants, J. Chem. Thermodyn. 42 (2010) 84-89.

[38] P. Gao, L.J. Meng, M.P. dos Santos, V. Teixeira, M. Andritschky, Study of ZrO_2–Y_2O_3 films prepared by rf magnetron reactive sputtering, Thin Solid Films 377-378 (2000) 32-36.

[39] S.N. Basahel, T.T. Ali, M. Mokhtar, K. Narasimharao, Influence of crystal structure of nanosized ZrO_2 on photocatalytic degradation of methyl orange, Nanoscale Res. Lett. 10:73 (2015).

[40] J.D. McCullough, K.N. Trueblood, The crystal structure of baddeleyite (monoclinic ZrO_2), Acta Crystallogr. 12 (1959) 507-511.

[41] Y.-l. Su, J. Wang, H.-z. Liu, FTIR Spectroscopic Study on Effects of Temperature and Polymer Composition on the Structural Properties of PEO−PPO−PEO Block Copolymer Micelles, Langmuir 18 (2002) 5370-5374.

[42] B. Tang, C. Wu, M. Qiu, X. Zhang, S. Zhang, PEG/SiO_2–Al_2O_3 hybrid form-stable phase change materials with enhanced thermal conductivity, Mat. Chem. Phys. 144 (2014) 162-167.

[43] H. Lai, Z. Wang, P. Wu, B.I. Chaudhary, S.S. Sengupta, J.M. Cogen, B. Li, Structure and Diffusion Behavior of Trioctyl Trimellitate (TOTM) in PVC Film Studied by ATR-IR Spectroscopy, Ind. Eng. Chem. Res. 51 (2012) 9365-9375.

[44] S. Pramanik, K. Sagar, B.K. Konwar, N. Karak, Synthesis, characterization and properties of a castor oil modified biodegradable poly(ester amide) resin, Prog. Org. Coat. 75 (2012) 569-578.

[45] I. Otero, E.R. López, M. Reichelt, M. Villanueva, J. Salgado, J. Fernández, Ionic Liquids Based on Phosphonium Cations As Neat Lubricants or Lubricant Additives for a Steel/Steel Contact, ACS Appl. Mat. Inter. 6 (2014) 13115-13128.

[46] X. Paredes, Viscous Behaviour of Lubricants at High Pressures, Thesis, University of Santiago de Compostela (2012)

[47] S. Mia, N. Ohno, Relation between low temperature fluidity and sound velocity of lubricating oil, Tribol. Int. 43 (2010) 1043-1047.

[48] N. Ohno, M.Z. Rahman, K. Kakuda, Bulk Modulus of Lubricating Oils as Predominant Factor Affecting Tractional Behavior in High-Pressure Elastohydrodynamic Contacts, Tribol. Trans. 48 (2005) 165-170.

[49] S. Mia, Prediction of Tribological and Rheological Properties of Lubricating Oils by Sound Velocity, Saga University (2010)

[50] A. Hernández Battez, J. Viesca, R. González Rodríguez, A. García Martínez, T. Reddyhoff, A. Higuera-Garrido, Effect of Shear Rate, Temperature, and Particle Concentration on the Rheological Properties of ZnO and ZrO_2 Nanofluids, Tribol. Trans. 57 (2014) 489-495.

[51] J. Meyer, S. Adio, M. Sharifpur, P. N. Nwosu, The Viscosity of Nanofluids: A Review of the Theoretical, Empirical, and Numerical Models, Heat Transfer Eng. 37 (2016) 387-421.

[52] X. Paredes, A.S. Pensado, M.J.P. Comuñas, J. Fernández, How Pressure Affects the Dynamic Viscosities of Two Poly(propylene glycol) Dimethyl Ether Lubricants, J. Chem. Eng. Data 55 (2010) 4088-4094.

[53] M. Kole, T.K. Dey, Effect of aggregation on the viscosity of copper oxide-gear oil nanofluids, Int. J. Therm. Eng. 50 (2011) 1741-1747.

[54] B.C. Pak, Y.I. Cho, Hydrodynamic and heat transfer study of dispersed fluids with submicron metallic oxide particles, Exp. Heat Transf. Int. 11 (1998) 151-170.

[55] E.J. Wasp, J.P. Kenny, R.L. Gandhi, Solid-liquid flow slurry pipeline transportation, Ser Bulk Mater Handl 1:56-58 (1977).

[56] A. Kotia, A. Haldar, R. Kumar, P. Deval, S.K. Ghosh, Effect of copper oxide nanoparticles on thermophysical properties of hydraulic oil-based nanolubricants, J. Braz. Soc. Mec. Sci. Eng. 39 (2017) 259-266.

[57] D. Cabaleiro, M.J. Pastoriza-Gallego, C. Gracia-Fernández, M.M. Piñeiro, L. Lugo, Rheological and volumetric properties of TiO_2-ethylene glycol nanofluids, Nanoscale Res. Lett. 8 (2013) 286-286.

[58] P.C. Mishra, S. Mukherjee, S.K. Nayak, A. Panda, A brief review on viscosity of nanofluids, Int. Nano Lett. 4 (2014) 109-120.

[59] A. Barati-Harooni, A. Najafi-Marghmaleki, A. Mohebbi, A.H. Mohammadi, On the estimation of viscosities of Newtonian nanofluids, J. Mol. Liquids 241 (2017) 1079-1090.

[60] G.K. Batchelor, The effect of Brownian motion on the bulk stress in a suspension of spherical particles, J. Fluid Mech. 83 (1977) 97-117.

[61] H.C. Brinkman, The Viscosity of Concentrated Suspensions and Solutions, J. Chem. Phys. 20 (1952) 571-571.

[62] A. Einstein, Eine neue bestimmung der moleküldimensionen, Annalen der Physik 324.2 (1906) 289-306.

[63] M.K. Meybodi, A. Daryasafar, M.M. Koochi, J. Moghadasi, R.B. Meybodi, A.K. Ghahfarokhi, A novel correlation approach for viscosity prediction of water based nanofluids of Al_2O_3, TiO_2, SiO_2 and CuO, J. Taiwan Inst. Chem.Eng. 58 (2016) 19-27.

[64] H. Chen, Y. Ding, C. Tan, Rheological behaviour of nanofluids, New J. Phys. 9 (2007) 367.

[65] N. Saitô, Concentration Dependence of the Viscosity of High Polymer Solutions. I, J. Phys. Soc. Japan 5 (1950) 4-8.

[66] X. Wang, X. Xu, S.U. S. Choi, Thermal Conductivity of Nanoparticle - Fluid Mixture, J. Thermophys. Heat Trans. 13 (1999) 474-480.

Table 1. Experimental densities, ρ/g·cm^{-3}, determined with both Stabinger and DSA 5000 densimeters for the synthetic oils used as base fluids at different temperatures and 0.1 MPa.

	Stabinger			*DSA*		
T (K)	*PAG2*	*TTM*	*BIOE*	*PAG2*	*TTM*	*BIOE*
278.15	1.0011	0.9642	0.9522			
283.15	0.9976	0.9609	0.9490	0.99847	0.96206	0.95029
288.15	0.9938	0.9576	0.9457	0.99455	0.95850	0.94682
293.15	0.9900	0.9542	0.9425	0.99069	0.95483	0.94330
298.15	0.9862	0.9509	0.9392	0.98683	0.95128	0.93975
303.15	0.9824	0.9475	0.9360	0.98297	0.94788	0.93644
308.15	0.9787	0.9442	0.9327	0.97911	0.94449	0.93314
313.15	0.9749	0.9408	0.9295	0.97525	0.94110	0.92984
318.15	0.9711	0.9375	0.9262	0.97141	0.93769	0.92655
323.15	0.9673	0.9342	0.9230	0.96759	0.93436	0.92326
328.15	0.9635	0.9309	0.9198	0.96377	0.93104	0.91997
333.15	0.9598	0.9276	0.9166	0.95997	0.92771	0.91674
338.15	0.9560	0.9242	0.9134	0.95618	0.92438	0.91352
343.15	0.9521	0.9209	0.9101			
348.15	0.9483	0.9176	0.9069			
353.15	0.9445	0.9142	0.9037			
358.15	0.9407	0.9109	0.9005			
363.15	0.9369	0.9076	0.8972			
368.15	0.9332	0.9042	0.8940			
373.15	0.9294	0.9009	0.8908			

Table 2. Experimental densities, ρ/g·cm^{-3}, determined with Stabinger densimeter for the nanolubricants at different temperatures and 0.1 MPa.

T/K	ρ/g·cm^{-3}	T/K	ρ/g·cm^{-3}	T/K	ρ/g·cm^{-3}
99 wt % PAG2 + 1 wt % ZrO_2					
278.15	1.0093	313.15	0.9829	348.15	0.9563
283.15	1.0054	318.15	0.9791	353.15	0.9525
288.15	1.0016	323.15	0.9753	358.15	0.9487
293.15	0.9981	328.15	0.9715	363.15	0.9449
298.15	0.9943	333.15	0.9677	368.15	0.9411
303.15	0.9905	338.15	0.9639	373.15	0.9373
308.15	0.9867	343.15	0.9601		
99 wt % TTM + 1 wt% ZrO_2					
278.15	0.9720	313.15	0.9487	348.15	0.9254
283.15	0.9688	318.15	0.9454	353.15	0.9221
288.15	0.9654	323.15	0.9421	358.15	0.9187
293.15	0.9621	328.15	0.9388	363.15	0.9154
298.15	0.9588	333.15	0.9354	368.15	0.9120
303.15	0.9554	338.15	0.9321	373.15	0.9087
308.15	0.9520	343.15	0.9288		
99 wt% BIOE + 1 wt% ZrO_2					
278.15	0.9610	313.15	0.9380	348.15	0.9151
283.15	0.9577	318.15	0.9347	353.15	0.9119
288.15	0.9544	323.15	0.9314	358.15	0.9087
293.15	0.9512	328.15	0.9281	363.15	0.9054
298.15	0.9479	333.15	0.9249	368.15	0.9022
303.15	0.9446	338.15	0.9216	373.15	0.8989
308.15	0.9413	343.15	0.9184		
98 wt % PAG2 + 2 wt % ZrO_2					
278.15	1.0175	313.15	0.9908	348.15	0.9639
283.15	1.0136	318.15	0.9870	353.15	0.9601
288.15	1.0097	323.15	0.9831	358.15	0.9563
293.15	1.0058	328.15	0.9793	363.15	0.9525
298.15	1.0020	333.15	0.9754	368.15	0.9487
303.15	0.9985	338.15	0.9716	373.15	0.9450
308.15	0.9947	343.15	0.9677		
98 wt % TTM + 2 wt % ZrO_2					
278.15	0.9798	313.15	0.9568	348.15	0.9335
283.15	0.9766	318.15	0.9535	353.15	0.9302
288.15	0.9733	323.15	0.9501	358.15	0.9268
293.15	0.9700	328.15	0.9468	363.15	0.9235
298.15	0.9668	333.15	0.9435	368.15	0.9202
303.15	0.9634	338.15	0.9402	373.15	0.9171
308.15	0.9601	343.15	0.9369		

Table 2. *Continued*

T/K	ρ/g·cm^{-3}	T/K	ρ/g·cm^{-3}	T/K	ρ/g·cm^{-3}
98 wt % BIOE + 2 wt % ZrO_2					
278.15	0.9695	313.15	0.9464	348.15	0.9235
283.15	-	318.15	0.9431	353.15	0.9202
288.15	0.9630	323.15	0.9398	358.15	0.9170
293.15	0.9597	328.15	0.9366	363.15	0.9137
298.15	0.9564	333.15	0.9333	368.15	0.9104
303.15	0.9531	338.15	0.9300	373.15	0.9072
308.15	0.9498	343.15	0.9267		

Table 3. Experimental densities, ρ/g·cm^{-3}, determined with DSA 5000 for the nanolubricants at different temperatures and 0.1 MPa.

T/K	ρ/g·cm^{-3}	T/K	ρ/g·cm^{-3}	T/K	ρ/g·cm^{-3}
		99 wt % PAG2 + 1 wt % ZrO_2			
283.15	1.00650	303.15	0.99089	323.15	0.97542
288.15	1.00252	308.15	0.98701	328.15	0.97157
293.15	0.99865	313.15	0.98314	333.15	0.96773
298.15	0.99477	318.15	0.97927	338.15	0.96391
		99 wt % TTM + 1 wt % ZrO_2			
283.15	0.97031	303.15	0.95603	323.15	0.94243
288.15	0.96673	308.15	0.95262	328.15	0.93910
293.15	0.96304	313.15	0.94921	333.15	0.93576
298.15	0.95945	318.15	0.94579	338.15	0.93242
		99 wt % BIOE + 1 wt % ZrO_2			
283.15	0.95829	303.15	0.94436	323.15	0.93112
288.15	0.95481	308.15	0.94104	328.15	0.92781
293.15	0.95127	313.15	0.93773	333.15	0.92455
298.15	0.94769	318.15	0.93442	338.15	0.92133
		98 wt % PAG2 + 2 wt % ZrO_2			
283.15	1.00650	303.15	0.99089	323.15	0.97542
288.15	1.00252	308.15	0.98701	328.15	0.97157
293.15	0.99865	313.15	0.98314	333.15	0.96773
298.15	0.99477	318.15	0.97927	338.15	0.96391
		98 wt % TTM+ 2 wt% ZrO_2			
283.15	0.97031	303.15	0.95603	323.15	0.94243
288.15	0.96673	308.15	0.95262	328.15	0.93910
293.15	0.96304	313.15	0.94921	333.15	0.93576
298.15	0.95945	318.15	0.94579	338.15	0.93242
		98 wt % BIOE + 2 wt % ZrO_2			
283.15	0.95829	303.15	0.94436	323.15	0.93112
288.15	0.95481	308.15	0.94104	328.15	0.92781
293.15	0.95127	313.15	0.93773	333.15	0.92455
298.15	0.94769	318.15	0.93442	338.15	0.92133

Table 4. Experimental sound velocities, u/m·s^{-1}, determined with DSA 5000 for the synthetic oils used as base fluids at different temperatures and 0.1 MPa

T/K	u/m·s^{-1}	T/K	u/m·s^{-1}	T/K	u/m·s^{-1}
		PAG2			
283.15	1381.9	303.15	1315.0	323.15	1250.7
288.15	1364.8	308.15	1298.3	328.15	1235.3
293.15	1348.0	313.15	1282.2	333.15	1220.0
298.15	1331.3	318.15	1266.4	338.15	1204.9
		TTM			
283.15	1508.3	303.15	1416.0	323.15	1346.3
288.15	1480.6	308.15	1397.6	328.15	1330.2
293.15	1456.9	313.15	1380.2	333.15	1314.3
298.15	1435.6	318.15	1363.3	338.15	1298.7
		BIOE			
283.15	1523.0	303.15	1448.2	323.15	1382.1
288.15	1503.0	308.15	1431.1	328.15	1366.3
293.15	1484.0	313.15	1414.4	333.15	1350.7
298.15	1465.8	318.15	1398.1	338.15	1335.4

Table 5. Experimental sound velocities, u/m·s^{-1}, determined with DSA 5000 for the nanolubricants at different temperatures and 0.1 MPa.

T/K	u/m·s^{-1}	T/K	u/m·s^{-1}	T/K	u/m·s^{-1}
99 wt % PAG2 + 1 wt % ZrO_2					
283.15	1372.4	303.15	1305.7	323.15	1242.6
288.15	1355.4	308.15	1289.6	328.15	1227.4
293.15	1338.6	313.15	1273.8	333.15	1212.3
298.15	1322.1	318.15	1258.1	338.15	1197.4
99 wt % TTM + 1 wt % ZrO_2					
283.15	1504.5	303.15	1411.7	323.15	1342.4
288.15	1476.7	308.15	1393.3	328.15	1326.4
293.15	1452.7	313.15	1375.7	333.15	1310.6
298.15	1431.3	318.15	1358.9	338.15	1295.2
99 wt % BIOE + 1 wt % ZrO_2					
283.15	1518.4	303.15	1443.6	323.15	1377.7
288.15	1498.3	308.15	1426.6	328.15	1362.0
293.15	1479.4	313.15	1410.0	333.15	1346.6
298.15	1461.2	318.15	1393.7	338.15	1331.4
98 wt % PAG2 + 2 wt % ZrO_2					
283.15	1367.6	303.15	1301.0	323.15	1238.0
288.15	1350.6	308.15	1284.9	328.15	1222.8
293.15	1333.9	313.15	1269.0	333.15	1207.7
298.15	1317.3	318.15	1253.4	338.15	1192.9
98 wt % TTM + 2 wt% ZrO_2					
283.15	1499.8	303.15	1407.0	323.15	1337.7
288.15	1472.1	308.15	1388.6	328.15	1321.7
293.15	1448.0	313.15	1371.0	333.15	1305.9
298.15	1426.6	318.15	1354.2	338.15	1290.5
98 wt % BIOE + 2 wt % ZrO_2					
283.15	1512.5	303.15	1437.8	323.15	1372.0
288.15	1492.5	308.15	1420.8	328.15	1356.4
293.15	1473.5	313.15	1404.2	333.15	1340.9
298.15	1455.3	318.15	1388.0	338.15	1325.6

Table 6. Experimental viscosities, η/mPa·s, determined with Stabinger rotational viscometer for the synthetic oils used as base fluids at different temperatures and 0.1 MPa.

T/K	η/mPa·s	T/K	η/mPa·s	T/K	η/mPa·s
			PAG2		
278.15	351.0	313.15	58.66	348.15	20.33
283.15	252.7	318.15	48.83	353.15	18.06
288.15	187.7	323.15	41.17	358.15	16.14
293.15	143.0	328.15	35.10	363.15	14.51
298.15	111.3	333.15	30.23	368.15	13.11
303.15	88.40	338.15	26.27	373.15	11.89
308.15	71.44	343.15	23.02		
			TTM		
278.15	6609	313.15	300.4	348.15	45.83
283.15	3819	318.15	216.5	353.15	37.38
288.15	2313	323.15	159.6	358.15	30.87
293.15	1449	328.15	120.1	363.15	25.78
298.15	936.3	333.15	92.05	368.15	21.77
303.15	623.3	338.15	71.83	373.15	18.55
308.15	427.2	343.15	56.96		
			BIOE		
278.15	5554	313.15	462.4	348.15	94.95
283.15	3579	318.15	353.2	353.15	79.47
288.15	2400	323.15	274.2	358.15	67.13
293.15	1652	328.15	216.1	363.15	57.21
298.15	1163	333.15	172.8	368.15	49.15
303.15	837.9	338.15	139.9	373.15	42.55
308.15	616.6	343.15	114.6		

Table 7. Experimental viscosities, η/mPa·s, determined with Stabinger rotational viscometer for nanolubricants at different temperatures and 0.1 MPa.

T/K	η/mPa·s	T/K	η/mPa·s	T/K	η/mPa·s
99 wt % PAG2 + 1 wt % ZrO_2					
278.15	358.9	313.15	59.77	348.15	20.76
283.15	258.3	318.15	49.76	353.15	18.46
288.15	191.8	323.15	41.96	358.15	16.51
293.15	146.1	328.15	35.79	363.15	14.85
298.15	113.6	333.15	30.83	368.15	13.43
303.15	90.17	338.15	26.81	373.15	12.20
308.15	72.83	343.15	23.50		
99 wt % TTM + 1 wt % ZrO_2					
278.15	6931	313.15	312.8	348.15	47.61
283.15	3997	318.15	225.0	353.15	38.84
288.15	2417	323.15	165.6	358.15	32.08
293.15	1515	328.15	124.6	363.15	26.79
298.15	977.8	333.15	95.60	368.15	22.62
303.15	650.8	338.15	74.60	373.15	19.27
308.15	445.3	343.15	59.16		
99 wt % BIOE + 1 wt % ZrO_2					
278.15	5803	313.15	478.98	348.15	97.54
283.15	3747	318.15	365.40	353.15	81.56
288.15	2504	323.15	283.33	358.15	68.85
293.15	1719	328.15	223.03	363.15	58.63
298.15	1209	333.15	178.05	368.15	50.35
303.15	869.77	338.15	144.00	373.15	43.56
308.15	639.22	343.15	117.86		
98 wt % PAG2 + 2 wt % ZrO_2					
278.15	365.6	313.15	60.70	348.15	21.17
283.15	263.0	318.15	50.59	353.15	18.81
288.15	195.1	323.15	42.69	358.15	16.83
293.15	148.4	328.15	36.43	363.15	15.15
298.15	115.3	333.15	31.40	368.15	13.69
303.15	91.46	338.15	27.31	373.15	12.44
308.15	73.89	343.15	23.95		
98 wt % TTM+ 2 wt % ZrO_2					
278.15	7151	313.15	320.1	348.15	48.56
283.15	4109	318.15	230.0	353.15	39.61
288.15	2482	323.15	169.1	358.15	32.70
293.15	1554	328.15	127.1	363.15	27.31
298.15	1003	333.15	97.50	368.15	23.05
303.15	667.6	338.15	76.10	373.15	19.65
308.15	456.4	343.15	60.36		

Table 7. *Continued*.

T/K	*η*/mPa·s	*T*/K	*η*/mPa·s	*T*/K	*η*/mPa·s
98 wt % BIOE + 2 wt % ZrO_2					
283.15	5850	313.15	481.5	348.15	98.17
288.15	-	318.15	367.3	353.15	82.09
293.15	2512	323.15	284.9	358.15	69.30
298.15	1725	328.15	224.4	363.15	59.03
303.15	1214	333.15	179.2	368.15	50.71
308.15	873.7	338.15	144.9	373.15	43.86
278.15	642.4	343.15	118.6		

Table 8. Parameters of Eq. (2) and average absolute deviation (AAD%) between experimental and correlated values for each base oil and nanolubricant.

Sample	***A* / mPa·s^{-1}**	***B* / K**	***C* / K**	**AAD%**
PAG2 base oil	0.32487	710.02	176.50	0.2
99 wt % PAG2 + 1 wt % ZrO_2	0.33250	708.60	176.70	0.1
98 wt % PAG2 + 2 wt % ZrO_2	0.35400	696.40	177.80	0.2
TTM base oil	0.00876	1603.9	159.64	3.4
99 wt % TTM + 1 wt % ZrO_2	0.00836	1625.0	158.91	3.7
98 wt % TTM + 2 wt % ZrO_2	0.01131	1549.1	162.18	2.6
BIOE base oil	0.06050	1440.7	152.07	0.9
99 wt % BIOE + 1 wt % ZrO_2	0.05600	1469.2	150.92	1.0
98 wt % BIOE + 2 wt % ZrO_2	0.06520	1425.2	153.18	0.7

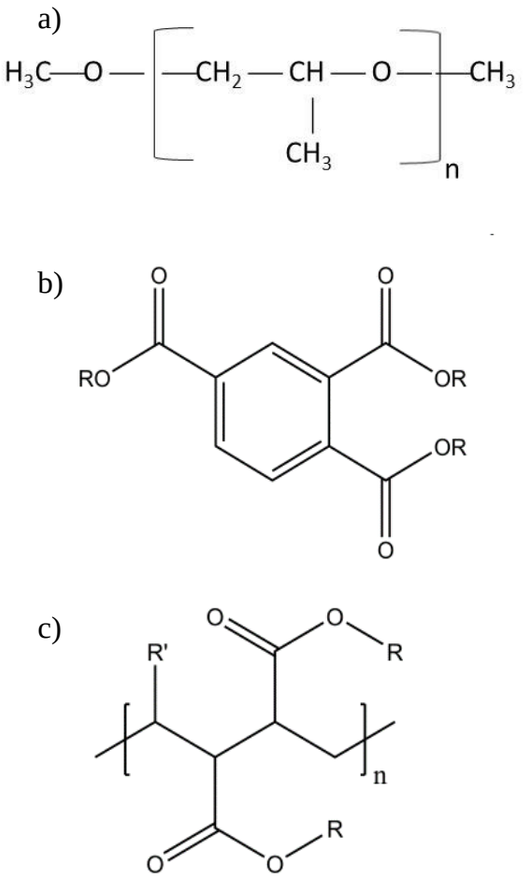

Figure 1. Chemical structures of the synthetic base oils: a) PAG2 (dimethoxy-end-capped poly(propylene glycol)), b) TTM (isotridecyl trimellitate ester) and c) BIOE (biodegradable polymeric ester). R represents alkyl groups.

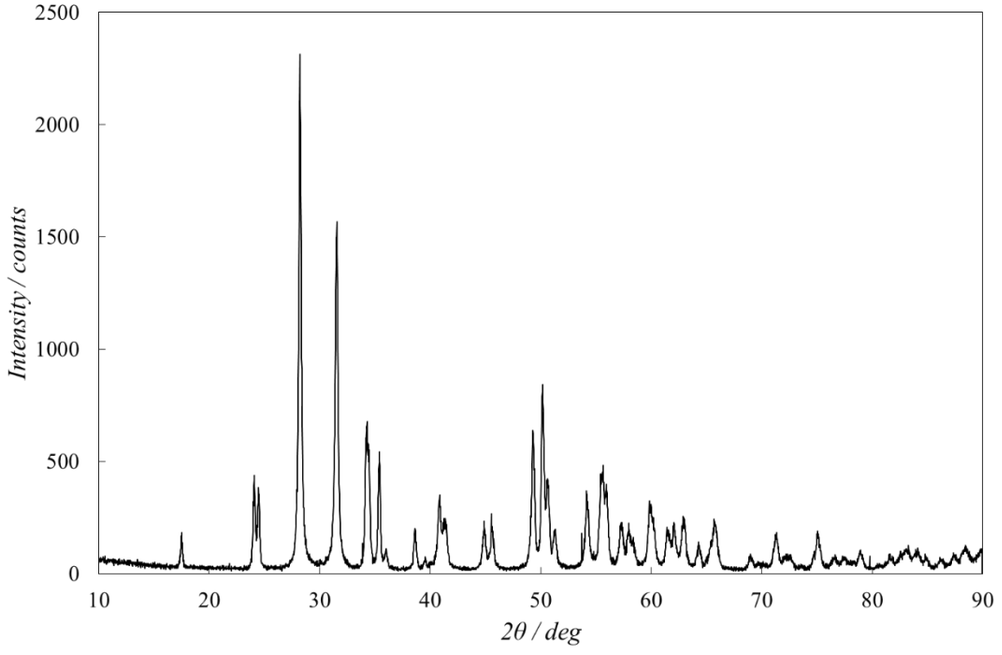

Figure 2. X-ray patterns of ZrO_2 nanopowder.

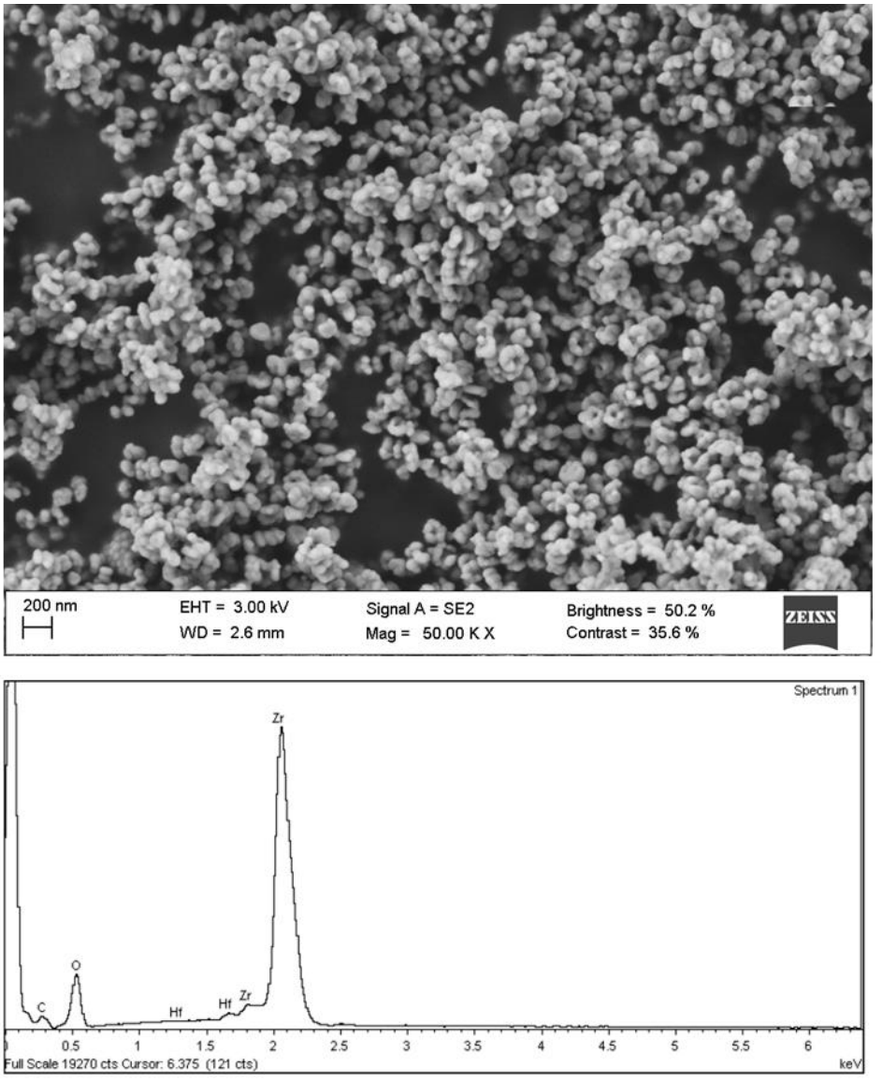

Figure 3. SEM micrograph and EDX microanalysis of spherically shaped ZrO_2 nanoparticles.

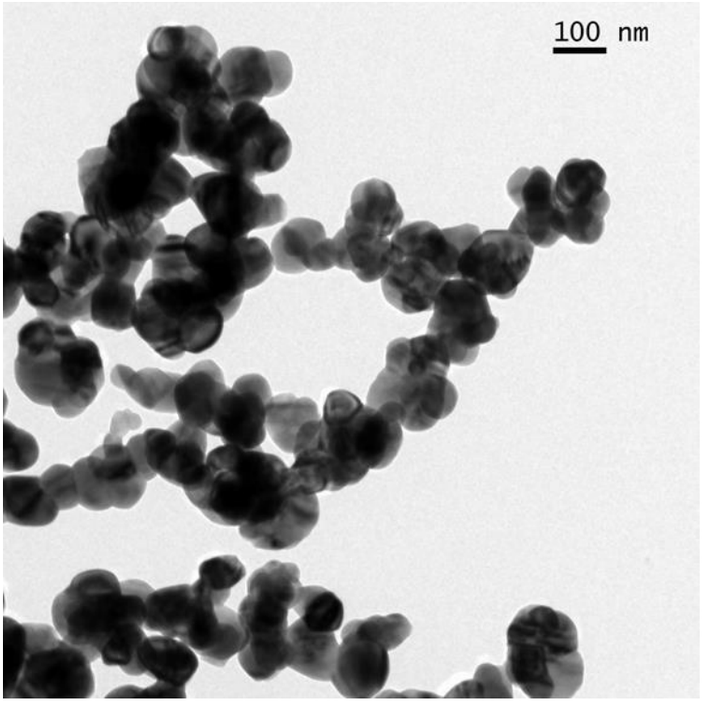

Figure **4**. TEM image of ZrO_2 nanoparticles dispersed in butanol.

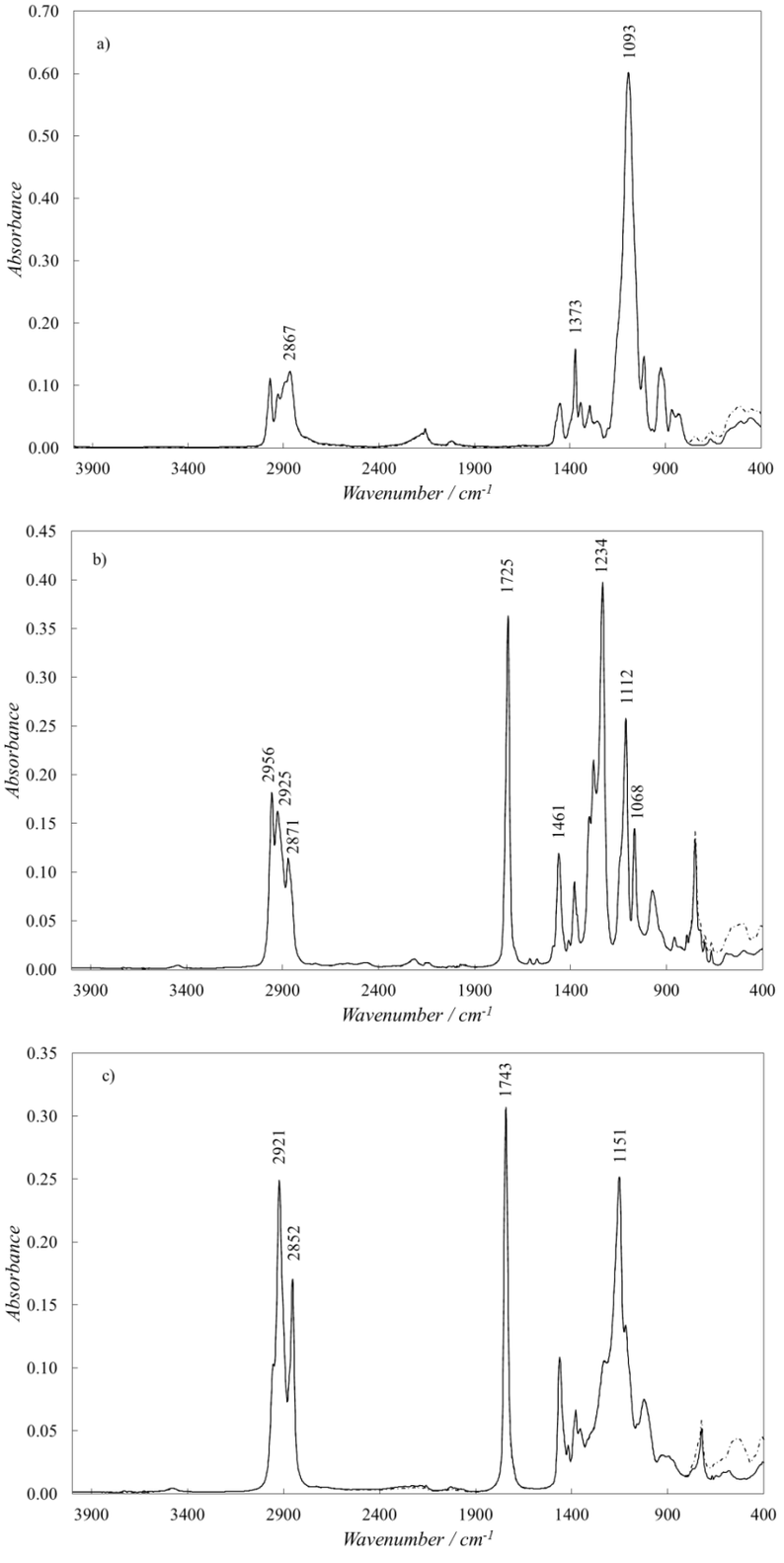

Figure 5. FTIR spectra of base oils (——) and nanolubricants with 2 wt% of ZrO_2 nanoparticles (-·-·-·). a) PAG2, b) TTM and c) BIOE.

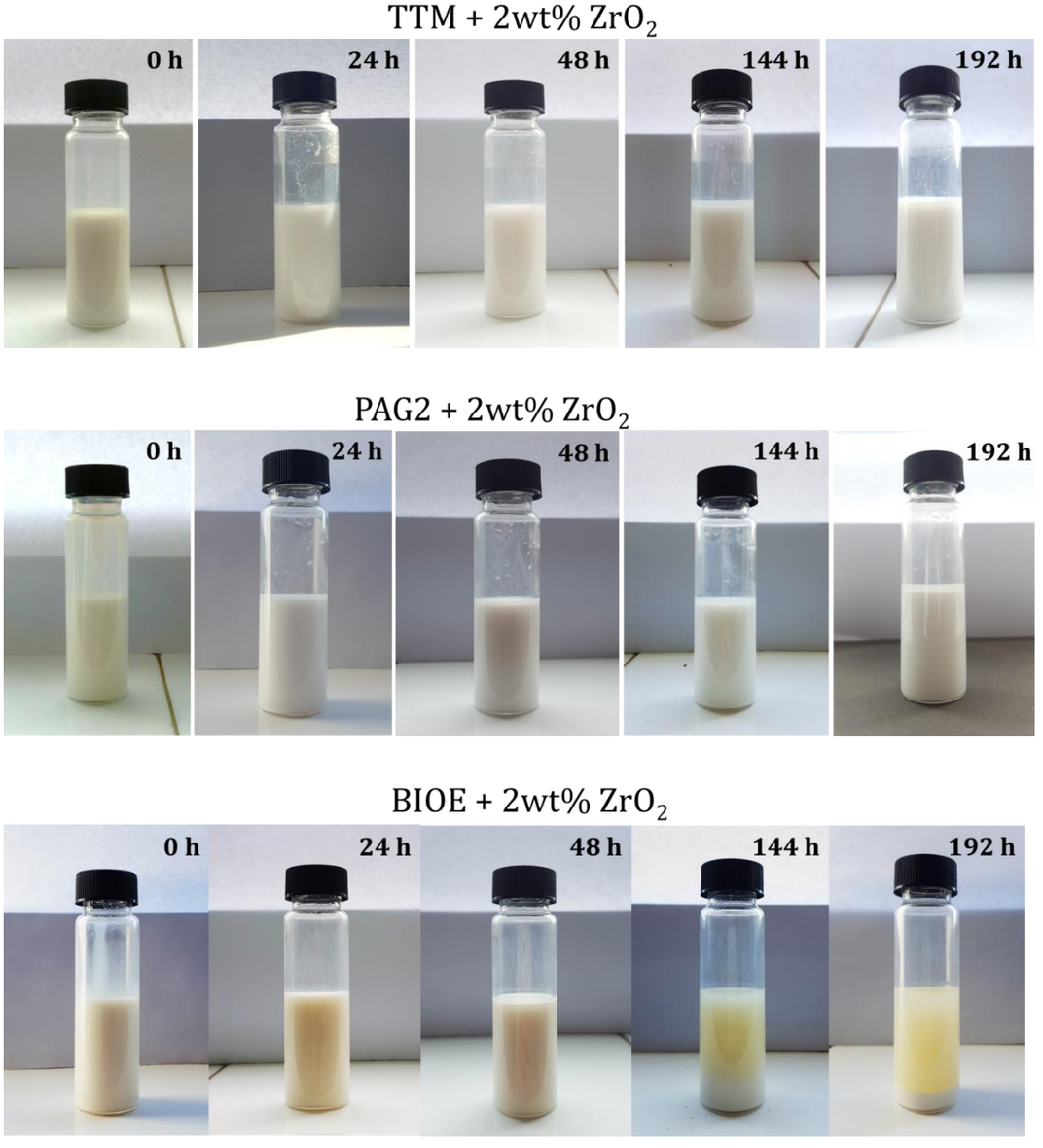

Figure 6. Photographs captured to observe the sedimentation of ZrO_2 nanoadditive at 2%wt mass concentration in PAG2, TTM and BIOE.

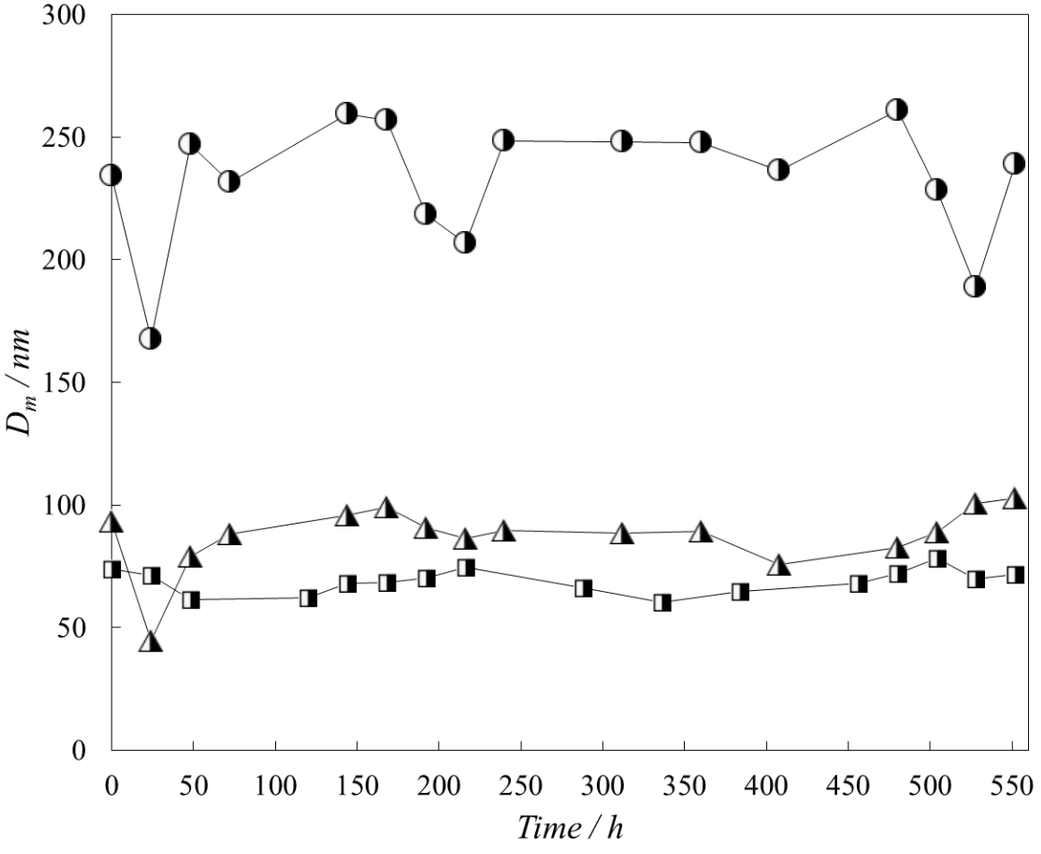

Figure 7. Average particle size diameter, D_m, obtained by DLS for dispersions at 2 wt% concentration of ZrO_2 nanoparticles in: (◑) PAG2; (◭) TTM and (◨) BIOE base oils.

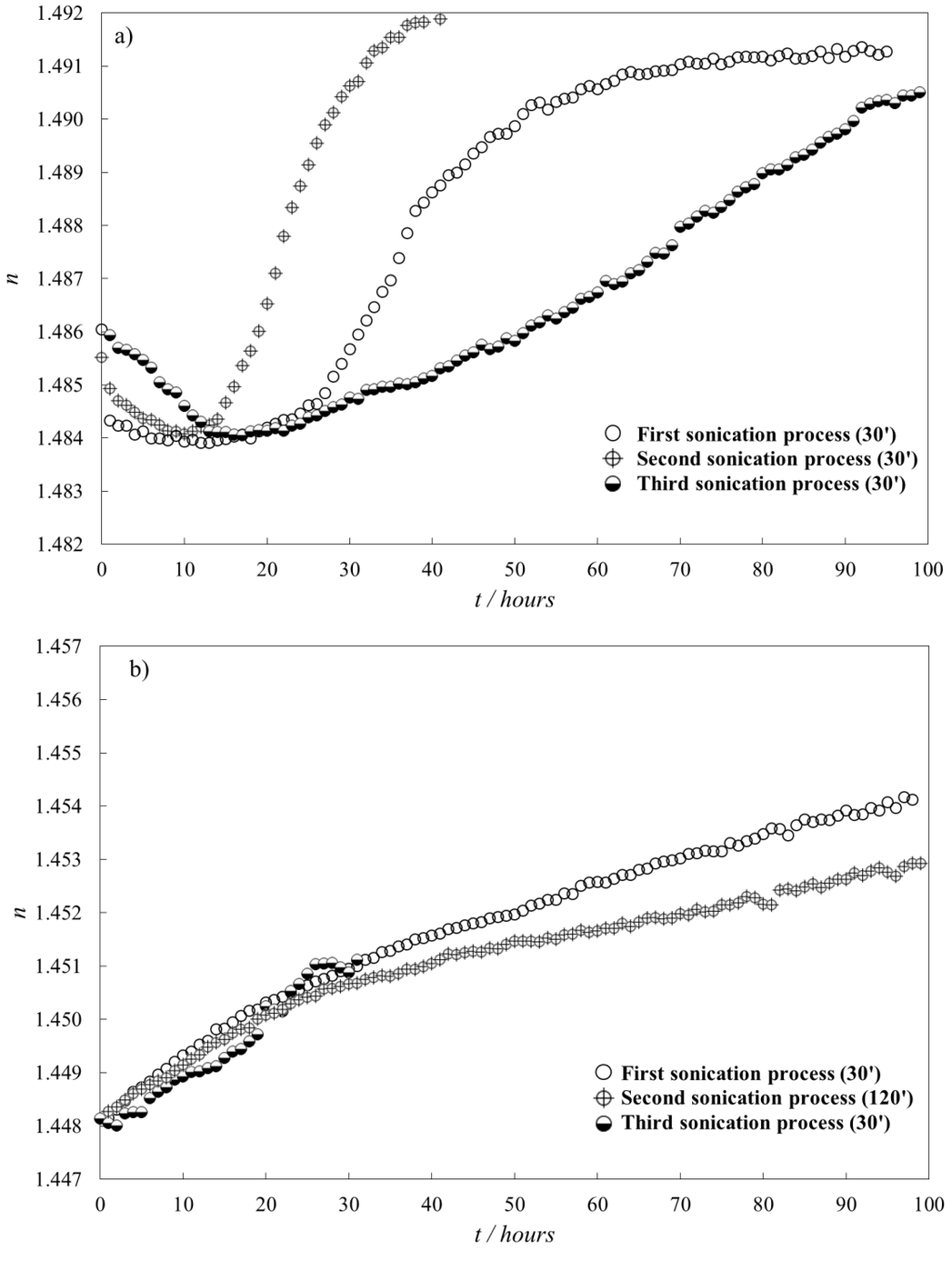

Figure 8. Temporal evolution of the refractive index, n, at 298.15 K for nanolubricants at 2 wt%. (a) ZrO_2/TTM and (b) ZrO_2/PAG2.

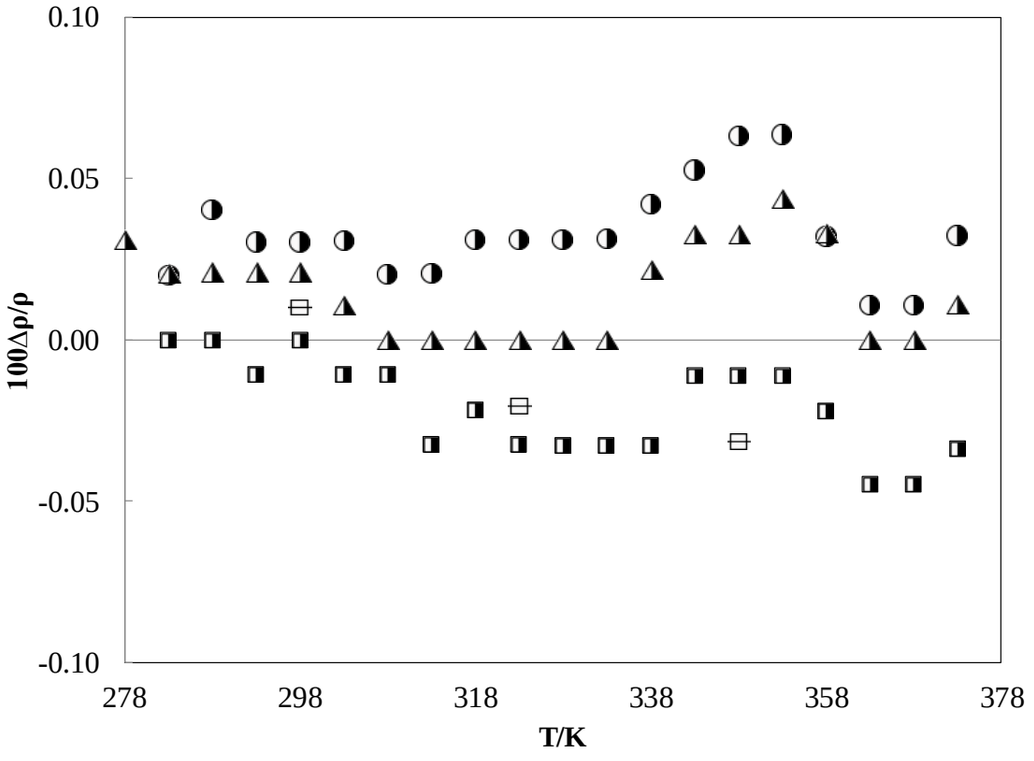

Figure 9. Relative deviation between densities obtained in this work for the base oils with Anton Paar SVM 3000 Stabinger and those previously reported by Otero et al. [45] for (◭) TTM and (◨) BIOE, by Paredes [46] for (◑) PAG2 and by Fandiño et al. [37] for (⊟) PAG2.

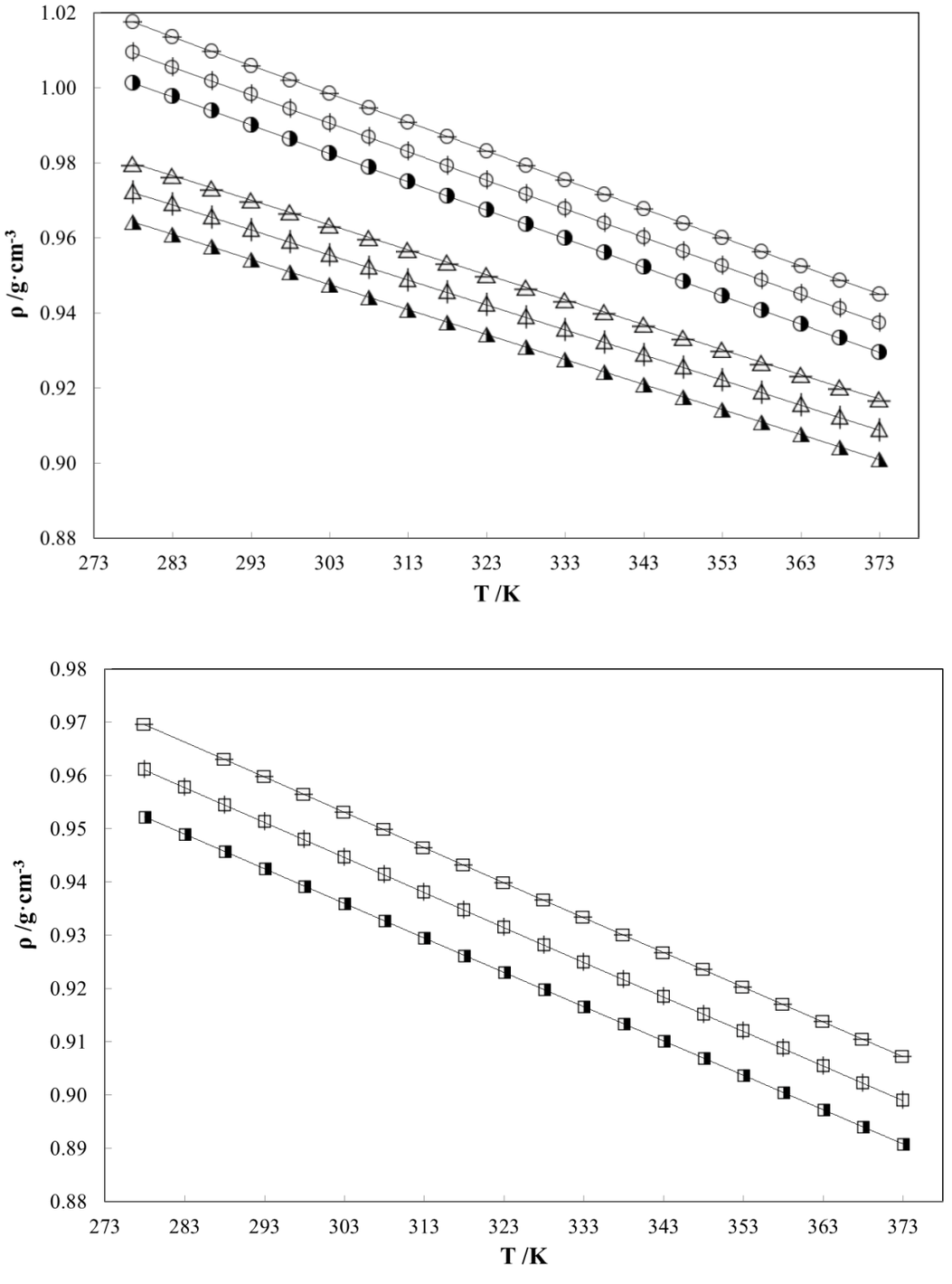

Figure 10. Densities, ρ, for each nanolubricant: (◑) PAG2 base oil; (⊕) PAG2 + 1.0 wt%; (⊖) PAG2 + 2.0 wt%; (◭) TTM base oil; (⧋) TTM + 1.0 wt%; (△) TTM + 2.0 wt%; (◨) BIOE base oil; (⊞) BIOE + 1.0 wt% and (⊟) BIOE + 2.0 wt%.

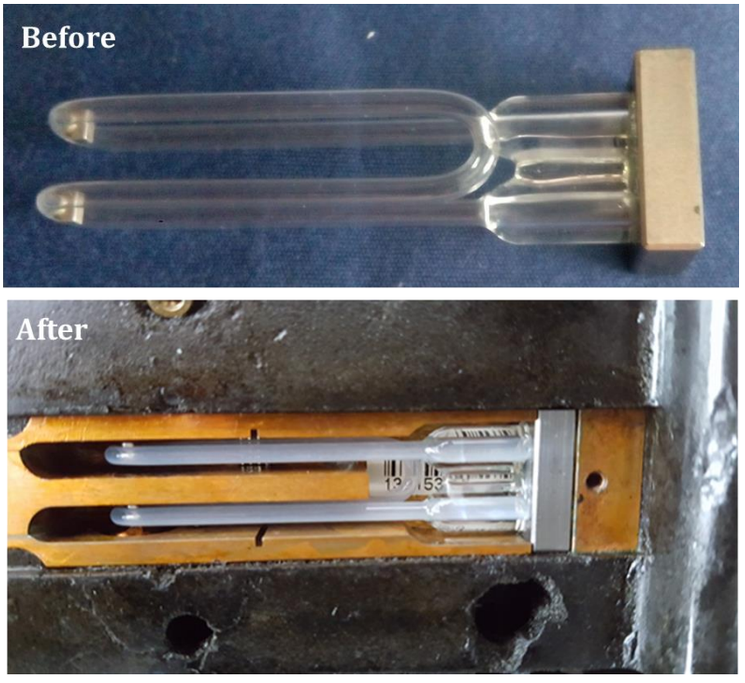

Figure 11. Stabinger SVM3000 densimeter cell before and after the density experiments with ZrO_2 nanoparticles.

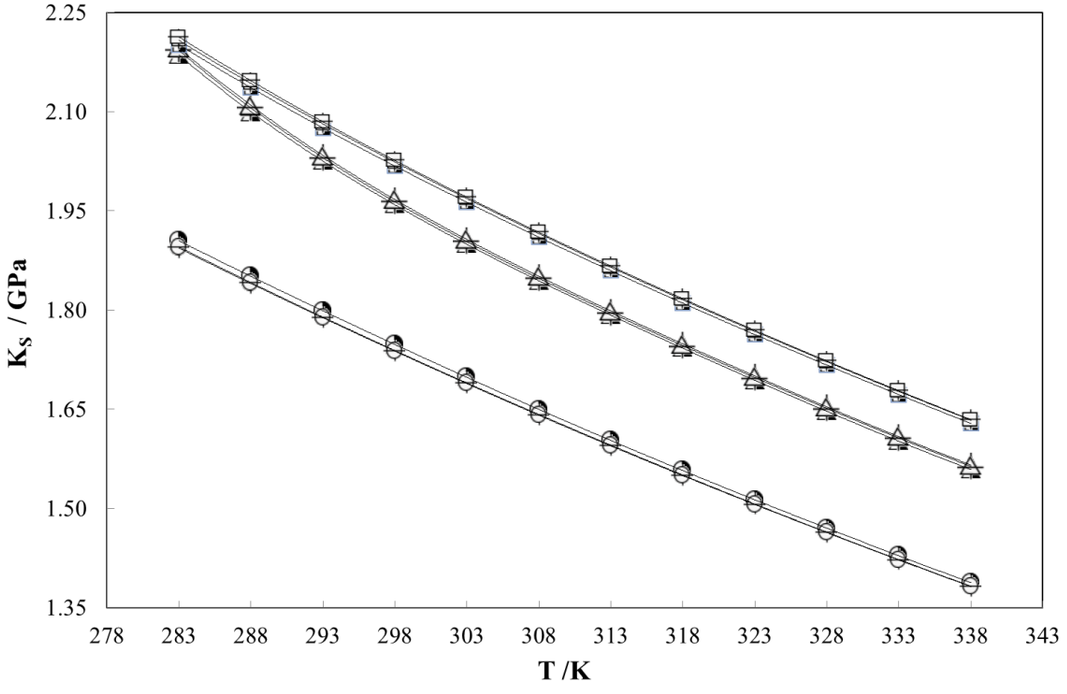

Figure 12. Adiabatic bulk modulus, K_s, for each nanolubricant as a function of the temperature: (◑) PAG2 base oil; (⌽) PAG2 + 1.0 wt %; (⊖) PAG2 + 2.0 wt%; (◭) TTM base oil; (⍋) TTM + 1.0 wt%; (⍙) TTM + 2.0 wt %; (◨) BIOE base oil; (⍈) BIOE + 1.0 wt% and (⍇) BIOE + 2.0 wt%.

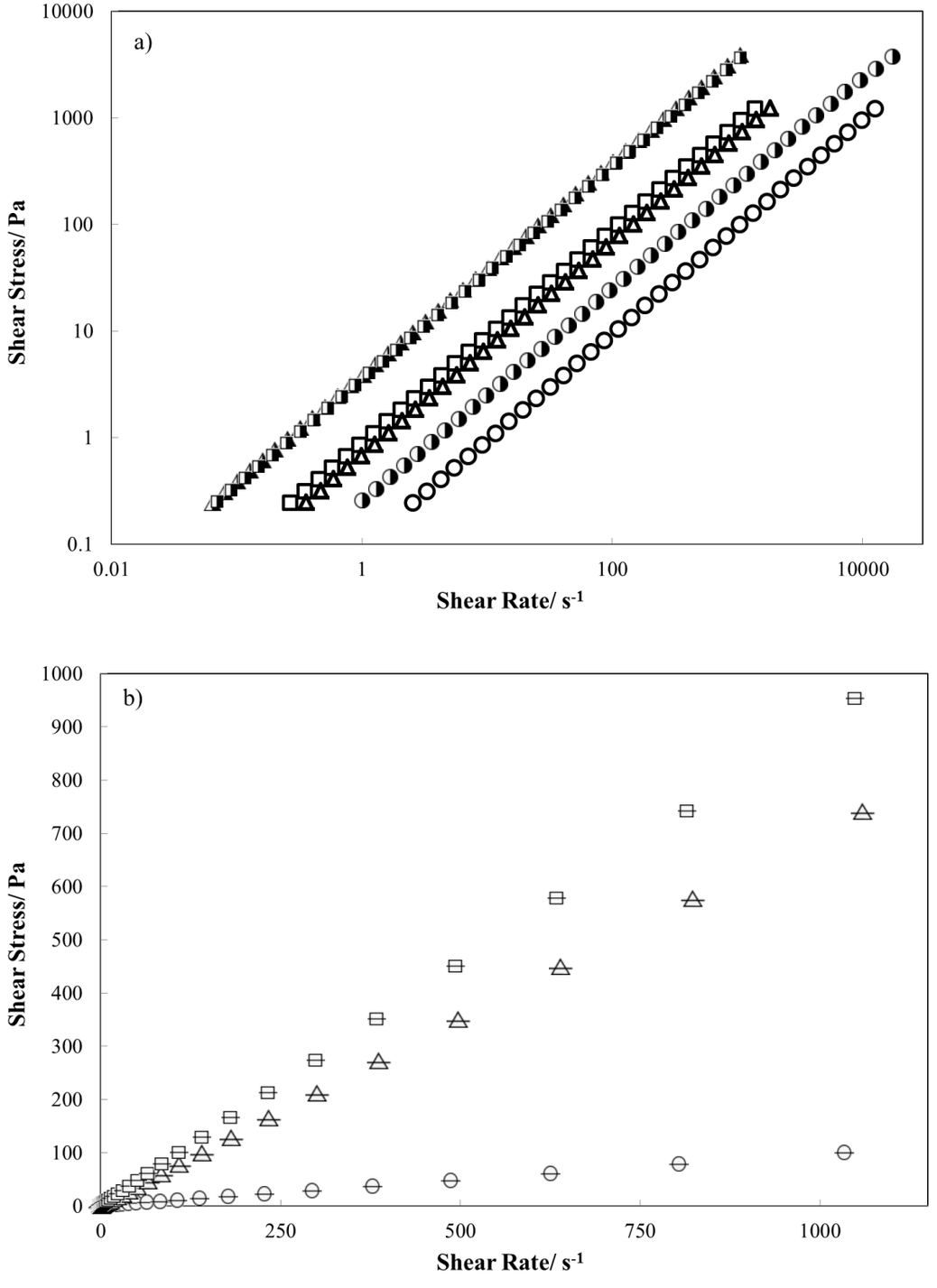

Figure 13. (a) Flow curves for the three base oils: PAG2 at (◑) 283.15 K and (○) 303.15 K; TTM at (◭) 283.15 K and (△) 303.15K; BIOE at (◨) 283.15 K and (◘) 303.15K. (b) Flow curves for nanolubricants based on (⊖) PAG2; (⧋) TTM and (⊟) BIOE at 2 wt% ZrO_2 concentration.

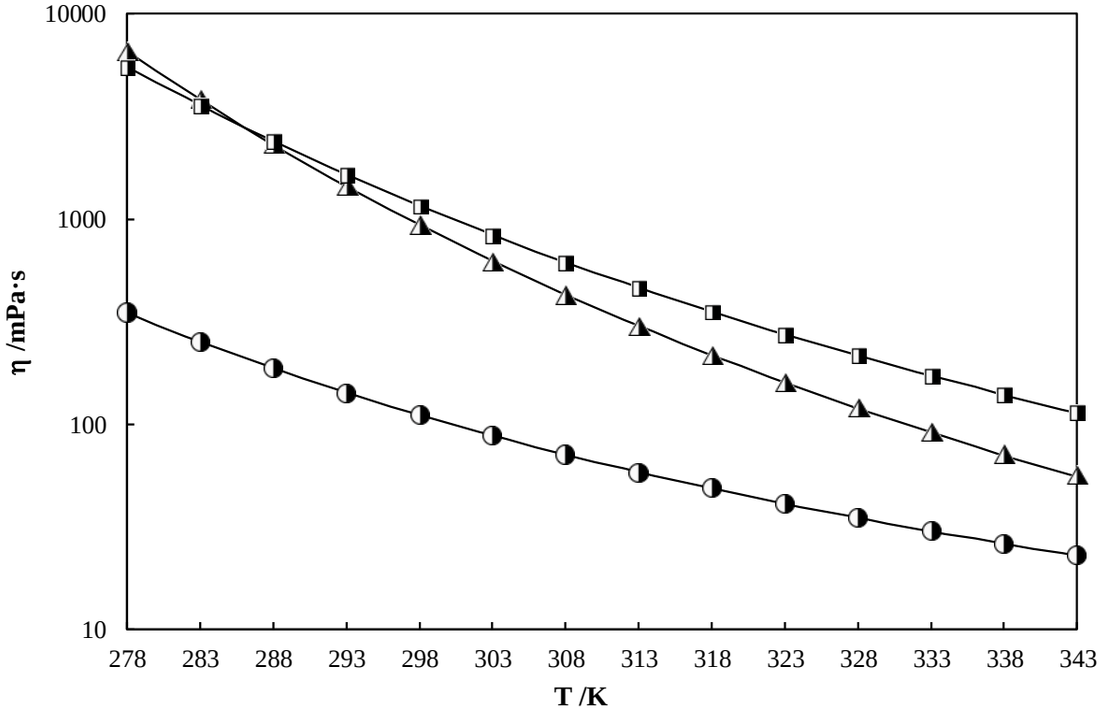

Figure 14. Dynamic viscosity (logarithmic scale) of the three base oils as a function of the temperature: (◑) PAG2; (◭) TTM and (◨) BIOE.

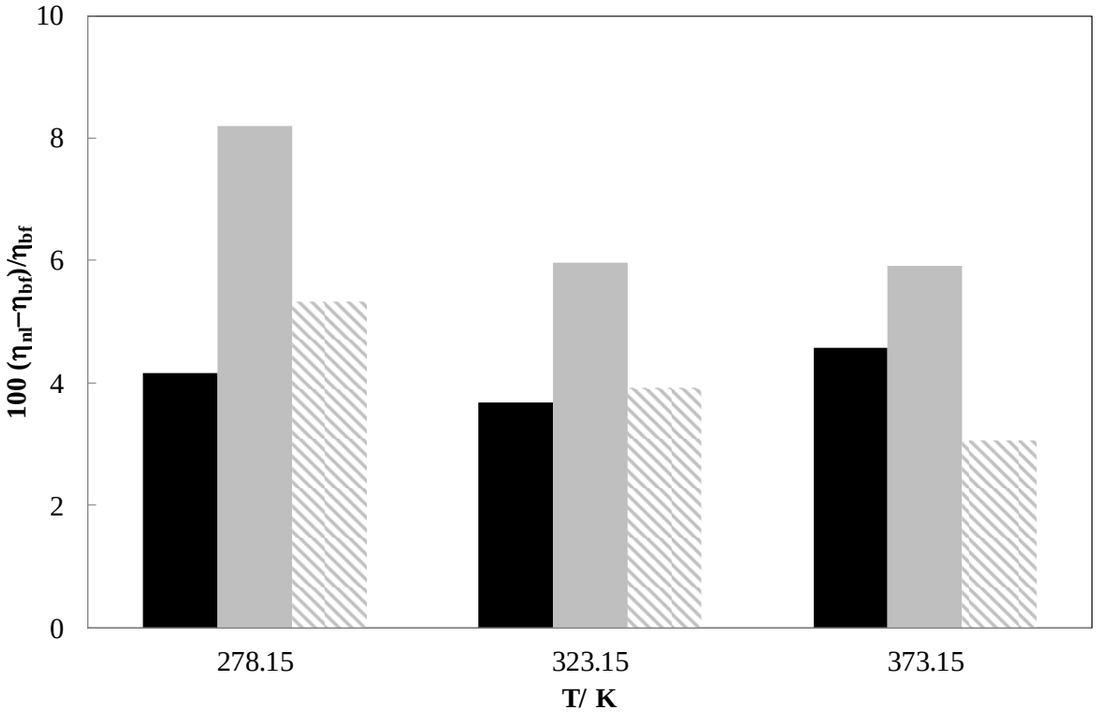

Figure 15. Relative variation of the viscosity of the nanolubricants of 2 wt% ZrO_2 concentration (η_{nl}) with respect to the base oil (η_{bf}): (■) PAG2; (▒) TTM and (▨) BIOE at 278.15 K, 323.15 K and 373.15K.

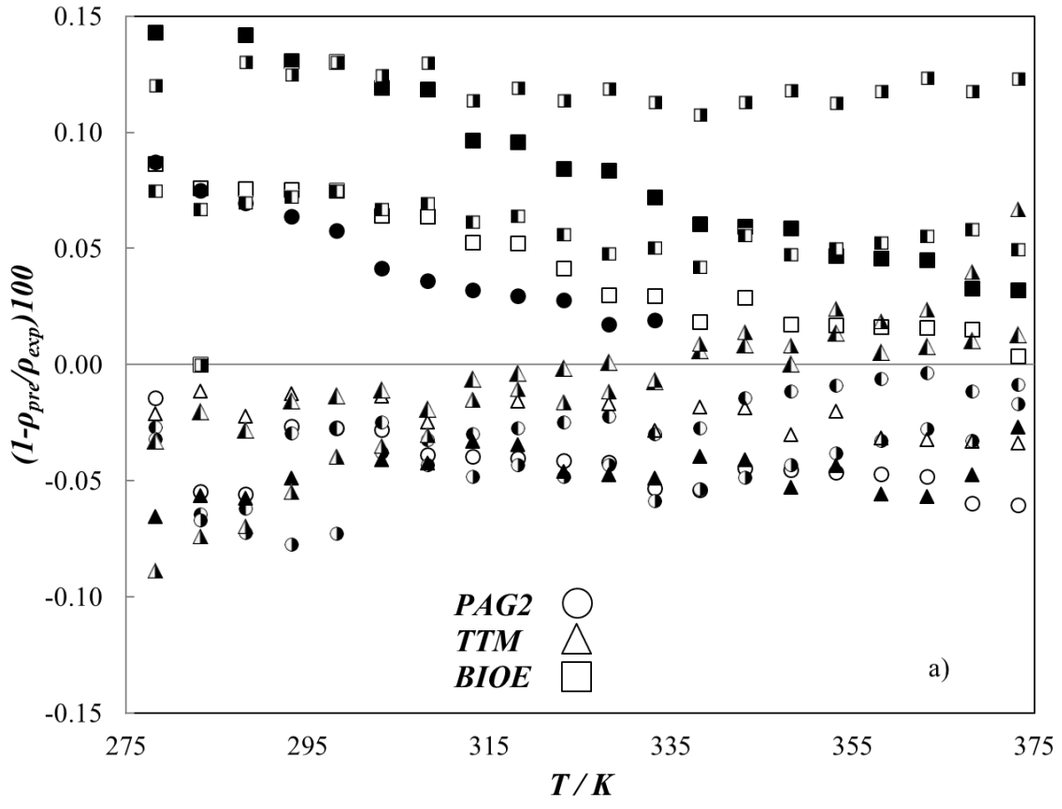

Figure 16. Relative deviations between experimental density data (ρ_{exp}) and predicted values (ρ_{pre}): (○; □; △) Pak and Cho [54] equation at 1 wt% ZrO_2; (●; ■; ▲) Pak and Cho [54] equation at 2 wt% ZrO_2, (◐; ◭; ◧) Wasp et al. [55] equation at 1 wt% ZrO_2 and , (◑; ◮; ◨) Wasp et al. [55] equation at 2 wt% ZrO_2.

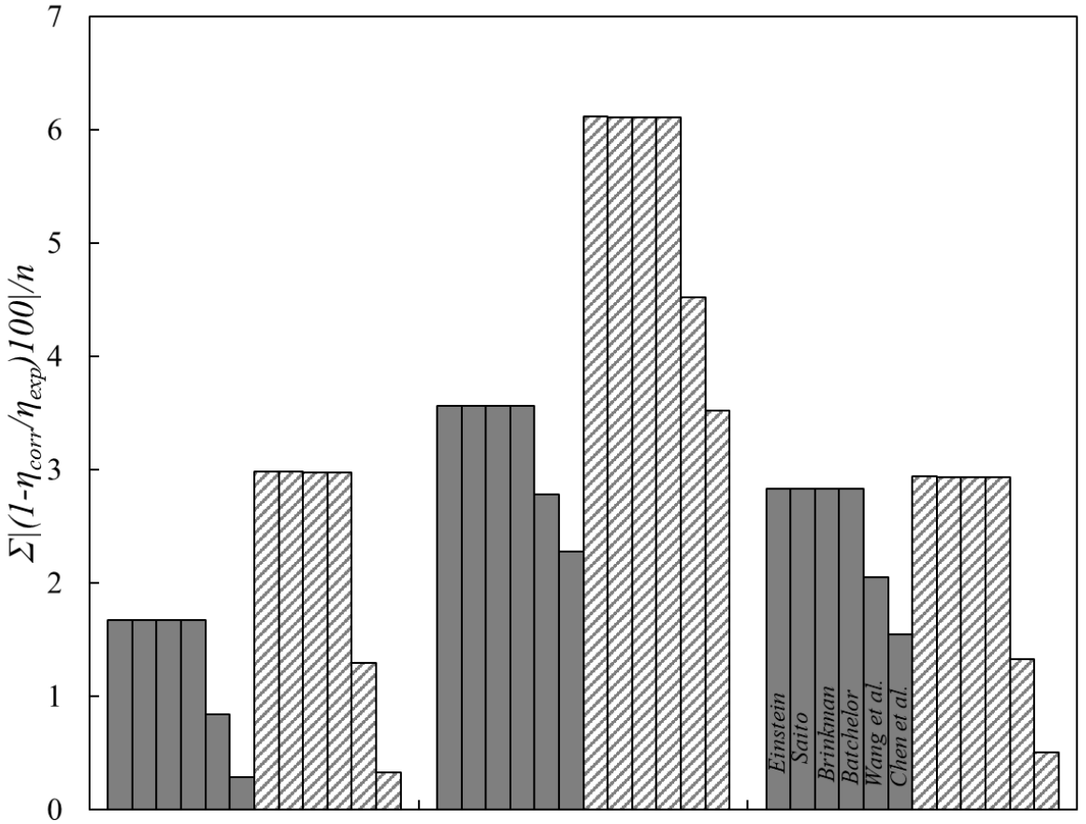

Figure 17. Absolute average relative deviations between experimental viscosity data (η_{exp}) and predicted values (η_{pre}) by using equations 5 to 10: (■) 1 wt% ZrO_2 and (▨) 2 wt% ZrO_2.